ORNL/TM-10339

ornl

OAK RIDGE NATIONAL LABORATORY

MARTIN MARIETTA

Changes in the Heating and Cooling Energy Use in Buildings Due to Lowering the Surface Solar Absorptance of Roofs

Edwin I. Griggs
George E. Courville

Part of
The National Program for
Building Thermal Envelope Systems
and Materials

Prepared for the
U.S. Department of Energy
Conservation and Renewable Energy
Office of Buildings and Community Systems
Building Systems Division

OPERATED BY
MARTIN MARIETTA ENERGY SYSTEMS, INC.
FOR THE UNITED STATES
DEPARTMENT OF ENERGY

Printed in the United States of America. Available from
National Technical Information Service
U.S. Department of Commerce
5285 Port Royal Road, Springfield, Virginia 22161
NTIS price codes—Printed Copy: A06; Microfiche A01

ORNL/TM-10339

CHANGES IN THE HEATING AND COOLING ENERGY USE IN BUILDINGS DUE TO LOWERING THE SURFACE SOLAR ABSORPTANCE OF ROOFS

Edwin I. Griggs

Tennessee Technological University
Cookeville, TN

and

George E. Courville

Energy Division
Oak Ridge National Laboratory
Oak Ridge, TN

Part of
The National Program for
Building Thermal Envelope Systems and Materials

Date Published - February 1989

Report Prepared by
Tennessee Technological University

for

Oak Ridge National Laboratory
Energy Division
Oak Ridge, TN
operated by

MARTIN MARIETTA ENERGY SYSTEMS, INC.
for the
U. S. DEPARTMENT OF ENERGY
under
Contract DE-AC05-84OR21400

TABLE OF CONTENTS

Section | Page

NOMENCLATURE

Symbol	Description	Units
A	Constant in h_o-wind speed correlation (see Equation C.1 in Appendix C)	Btu/hr-ft^2-F
ACE_1	Annual cooling energy per unit roof area for high roof α	Btu/ft^2
ACE_2	Annual cooling energy per unit roof area for low roof α	Btu/ft^2
ACES	Reduction in cooling energy per unit roof area following a discrete change in α	Btu/ft^2
AHE_1	Annual heating energy per unit roof area for high roof α	Btu/ft^2
AHE_2	Annual heating energy per unit roof area for low roof α	Btu/ft^2
AHEP	Increase in heating energy per unit roof area following a discrete change in α	Btu/ft^2
(ACES + AHEP)	Sum of annual cooling energy savings and annual heating energy penalties per unit roof area (represents reduced heat gain as manifested by effect on loads due to reducing roof's α)	Btu/ft^2
B	Constant in h_o-wind speed correlation (see Equation C.1 in Appendix C)	$\frac{\text{Btu-hr}}{\text{hr-ft}^2\text{-F-mi}}$
C	Constant in h_o-wind speed correlation (see Equation C.1 in Appendix C)	$\frac{\text{Btu-hr}^2}{\text{hr-ft-F-mi}^2}$
CDD	Designates cooling degree days	F
CEC	Cooling energy cost	¢/Btu
G	Incident solar radiation per unit roof area	$\frac{\text{Btu}}{\text{hr-ft}^2}$
$\overline{G}_{S_D}$	Mean daily solar radiation on a horizontal surface	$\frac{\text{Btu}}{\text{day-ft}^2}$
HDD	Designates heating degree days	F
h_e	External film heat transfer coefficient due solely to convection	$\frac{\text{Btu}}{\text{hr-ft}^2\text{-F}}$

Symbol	Description	Units
HEC	Heating energy costs	¢/Btu
h_i	Inside surface film heat transfer coefficient	$\frac{Btu}{hr\text{-}ft^2\text{-}F}$
h_o	Combined convective and radiative heat transfer coefficient ($h_e + h_r$)	$\frac{Btu}{hr\text{-}ft^2\text{-}F}$
h_r	Radiative heat transfer coefficient (see Equation 3.5)	$\frac{Btu}{hr\text{-}ft^2\text{-}F}$
PW	Present worth of an investment	¢/ft^2
$(PWF)_c$	Present worth factor applicable to energy used for cooling	---
$(PWF)_h$	Present worth factor applicable to energy used for heating	---
T_i	Conditioned space temperature	°F
T_o	Exterior roof surface temperature	°F or °R
T_{sa}	Sol-air temperature	°F
T_∞	Outside air temperature	°F or °R
U	Overall heat transfer coefficient (outside air to inside air)	$\frac{Btu}{hr\text{-}ft^2\text{-}F}$
U'	Heat transfer coefficient (outside surface to inside air)	$\frac{Btu}{hr\text{-}ft^2\text{-}F}$
U_o	Overall heat transfer coefficient (sol-air to inside air)	$\frac{Btu}{hr\text{-}ft^2\text{-}F}$
V	Wind speed	mi/hr
$\overline{V}$	Annual mean wind speed	mi/hr

Greek Symbol	Description	Units
α	Hemispherical surface absorptance	---
α_λ	Monochromatic absorptance	---
β	Cooling system coefficient of performance	---

Greek Symbol	Description	Units
ΔE	Difference between the energy emitted by a blackbody at T_∞ and the longwave radiation incident on a surface	$\frac{Btu}{hr\text{-}ft^2}$
ε	Infrared emittance	---
η	Heating system efficiency	---
ρ	Hemispherical surface reflectance	---
ρ_λ	Monochromatic reflectance	---
σ	Stefan-Boltzmann Constant (0.1714×10^{-8})	$\frac{Btu}{hr\text{-}ft^2\text{-}R^4}$
τ	Hemispherical transmittance	---
τ_λ	Monochromatic transmittance	---

LIST OF FIGURES

Figure | Page

LIST OF TABLES

Table		Page

FOREWORD

This is one of a series of reports to be published describing research, development, and demonstration activities in support of the National Program for Building Thermal Envelope Systems and Materials. The National Program involves several federal agencies and many other organizations in the public and private sectors who are addressing the national objective of decreasing energy wastes in the heating and cooling of buildings. Results described in this report are part of the National Program through delegation of management responsibilities for the DOE lead role to the Oak Ridge National Laboratory.

George E. Courville
Program Manager
Building Thermal Envelope
Systems and Materials
Oak Ridge National Laboratory

J. A. Smith
Program Manager, Director of Building
Systems
Office of Buildings and Community Systems
Department of Energy

BTESM REPORTS

C. SYSTEMS

1. LBL-8822: *A New Measurement Strategy for In-Situ Testing of Wall Thermal Performance* (March 1979).

2. LBL-9821: *Measurement of In-situ Dynamic Thermal Performance of Building Envelopes Using Heat Flow Meter Arrays* (December 1979).

3. NBS/BS Series 123: *The Effect of Moisture on the Thermal Conductance of Roofing Systems* (April 1980).

4. ORNL/Sub-78/97726/I: *A Field Study of Moisture Damage in Walls Insulated Without a Vapor Barrier* (May 1980).

5. ORNL/CON-46: *An Appraisal of the M Factor and the Role of Building Thermal Mass in Energy Conservation* (July 1980).

6. NBSIR 80-2100: *Thermal Resistance Measurements of a Built-Up Roof System* (October 1980).

7. ORNL/TR-4679: *Roofing Felt on Polystyrene* (December 1980).

8. ORNL/TM-7629: *Roofing Research – A Bibliography* (April 1981).

9. ORNL/TM-7640: *The Assessment of Roofing Research. An Interim Report* (July 1981).

10. *Southwest Thermal Mass Study, Tesuque Pueblo, New Mexico: Construction and Instrumentation Phase* (October 1981).

11. LBL-13436: *The Envelope Thermal Test Unit (ETTU): Field Measurement of Wall Performance* (October 1981).

12. LBL-13510: *The Determination of the Dynamic Performance of Walls* (November 1981).

13. LBL-13503: *Simplified Thermal Parameters: A Model of the Dynamic Performance of Wall* (December 1981).

14. NBSIR 81-2443: *Plan for A Round Robin of Hot Boxes* (February 1982).

15. CERL TR/M-308: *Insulation Retrofit Under Low-Slope Roofs* (February 1982).

16. CONF-811179: *Proceedings DOE-ORNL Workshop on Mathematical Modeling of Roofs, November 3–4, 1981, Atlanta, Georgia* (April 1982).

17. ORNL/Sub-42539/1: Heat Transfer Characteristics of a Structural Normal Weight Concrete Wall (February 1983).

18. ORNL/Sub-95006/1: *Thermal Roof Systems Performance Study* (March 1983).

19. ORNL/TM-8571: *Thermal Envelope Field Measurements in an Energy-Efficient Office and Dormitory* (April 1983).

20. ORNL/Sub-42539/2: *Heat Transfer Characteristics of a Structural Lightweight Concrete Wall* (June 1983).

21. CONF-8206130: *Proceedings of the Building Thermal Mass Seminar 1982* (August 1983).

22. ORNL/Sub-42539/3: *Heat Transfer Characteristics of a Low Density Concrete Wall* (August 1983).

23. ORNL/CON-97: *Thermal Mass Assessment* (September 1983).

24. ORNL/Sub-81-22293/1: *Energy Savings Potential of Roofing Research* (December 1983).

25. ORNL/Sub-7948/1: *Southwest Thermal Mass Study: The Effect of Envelope Thermal Mass On the Heating Energy Use of Eight Test Buildings In a High Desert Climate* (April 1984).

26. ORNL/TM-9004: *Economic Analyses of Insulation Materials Used in Low-Slope, Built-Up Roof Systems* (June 1984).

27. ORNL/CON-151: *Cooling Season Performance of an Earth Sheltered Office/Dormitory Building in Oak Ridge, Tennessee* (July 1984).

28. ORNL/Sub-7948/2: *Observation and Prediction of the Heating Season Thermal Mass Effect for Eight Test Buildings With and Without Windows* (September 1984).

29. ORNL/Sub-42539/4: *Calibrated Hot Box Test Results Data Manual* (November 1984).

30. ORNL/Sub-82-22293/2: *Roofing Industry Perspective and Research Capability* (March 1985).

31. ORNL/Sub-00240/1: *Assessment of the Energy Savings Potential of Building Foundation Research* (January 1985).

32. ORNL-6171: *Insulation System Basics for Built-Up Roof* (June 1985)

33. ORNL-6172: *Decision Guide for Roof Insulation R-Value* (June 1985)

34. ORNL/Sub-70376/1: *A Survey of Building Anomalies and Assessment of Thermal Break Materials for Anomaly Correction, Volume I - Survey and Assessment* (July 1985).

35. ORNL/Sub-70376/2: *A Survey of Building Anomalies and Assessment of Thermal Break Materials for Anomaly Correction, Volume II - Proceedings of the Federal Workshop on Building Envelope Thermal Anomalies* (July 1985).

36. ORNL-Sub-42539/5: *Calibrated Hot Box Test Results Data Manual, Volume II* (August 1985).

37. ORNL/CON-186: *Detailed Thermal Performance Measurements and Cost Effectiveness of Earth Sheltered Construction: A Case Study* (September 1985).

38. K/CSD/TM-56: *Analysis of Calibrated Hot Box Data for Three Concrete Walls* (September 1985).

39. K/CSD/TM-58: *The Use of Roof Temperature Modeling to Predict Necessary Conditions for Locating Wet Insulation with Infrared Thermography* (November 1985).

40. ORNL/CON-188: *Roof Test Center - A Preliminary Concept Paper* (November 1985).

41. ORNL/Sub-43122/1: *Mathematical Modeling of Whole Roof System Performance* (January 1986).

42. ORNL/Sub-43122/2: *Thermal and Hygric Roof (THR) Model Program* (January 1986).

43. ORNL/Sub-43122/3: *User's Manual for Program ROOF* (January 1986).

44. K/CSD/TM-59: *Calibration of Heat Flux Through a Wall Containing a Cavity - Comparison of Several Models* (February 1986).

45. NBSIR 86-3328: *The Assessment of Accuracy of In-Situ Methods for Measuring Building Envelope Thermal Resistance* (February 1986).

46. NBSIR 85-3264: *A Methodology for Assessing the Thermal Performance of Low-Sloped Roofing Systems* (May 1986).

47. ORNL/Sub-42539/7: *Surface Temperature Measurement Techniques For a Calibrated Hot Test Box Specimen* (June 1986).

48. ORNL/Sub-42539/6: *Heat Transfer Characteristics of Walls With Similar Thermal Resistance Values* (June 1986).

49. ORNL/Sub/85-27497/1: *Assessment of the Energy Savings Potential of Building Foundations Research, Summary Report* (November 1986).

50. ORNL/CON-222: *Building Foundations Research Agenda* (December 1986).

51. ORNL/Sub/83-70373/1: *Thermal Mass: BLAST Residential Parametric Simulations* (January 1987).

52. ORNL/Sub/83-70373/2: *Thermal Mass: A Comparison of Measurements and BLAST Predictions for Six Test Cells in Two Climates* (January 1987).

53. ORNL/Sub-21006/1: *Structural Thermal Break Systems for Buildings - Feasibility Study* (March 1987)

54. *The Roof Research Center - A National User Facility for Thermal Performance and Durability of Roofing Systems* (April 1987).

55. ORNL/Sub/85-27453/1: *Ultraviolet Radiation Testing of Roofing Systems* (July 1987).

56. ORNL/M-340: *Roofing Research Needs: An ORNL Draft Assessment* (August 1987).

57. CON-221: *Simulation of the SWTMS Test Cells Using the DOE-2.1A Model* (September 1987).

58. ORNL/Sub/79-42539/8: *Heat Transfer Characteristics of Insulated Concrete Sandwich Panel Walls* (September 1987).

59. ORNL/85-00294/1: *Building Envelope Thermal Anomaly Analysis* (December 1987).

60. ORNL/CON-245: *Impact of CFC Restrictions on U.S. Building Foundations Thermal Performance* (December 1987).

61. ORNL/Sub/86-72143/1: *Energy-Efficient Building Foundation Design Handbook* (May 1988).

62. ORNL/M-339: *Marketing Plan and Strategies - Roof Research Center* (June 1988).

63. ORNL/Sub/84-21006/2: *Structural Thermal Break Systems for Buildings - Development and Properties of Concrete Systems* (December 1988).

EXECUTIVE SUMMARY

OVERVIEW:

The radiative properties of a building's roof affect the heating and cooling loads imposed on the building's interior. With other factors being equal, a light-colored roof (i.e., one with a low solar absorptance) will be cooler than a dark-colored one during hours of solar exposure. Consequently, use of a light-colored roof in contrast to a dark-colored one will have a counteracting effect on annual energy use. Typically, the cooling requirements will decrease while heating requirements will increase. The distinction between these counteracting effects will vary with location. Questions regarding the preferable color of roof for a particular location prevail and their resolutions involve both technical and economic considerations.

In an effort to quantify potential energy savings resulting from the use of a flat roof having a low solar absorptance, an in-house study was undertaken with the Building Thermal Envelope Systems and Materials (BTESM) group within the Energy Division at Oak Ridge National Laboratory. The effort was a first step in addressing the issue and was to provide support for a complementary experimental program planned for the Roof Thermal Research Apparatus (RTRA) at ORNL.

SYNOPSIS:

Pertinent literature was reviewed, and the results and scope of other studies were summarized in establishing background for this work.

Fundamental concepts including the mathematical representation of an energy balance at the outer sunlit surface of a flat roof and the definition of sol-air temperature were summarized. The resulting expressions aid in showing how key parameters enter into the calculations.

The effort involved computing changes in a building's heating and cooling requirements caused by reducing the solar absorptance of its flat roof from 0.8 to 0.3. Computations were made using the computer code DOE 2.1B principally because of its inclusion of dynamic effects and HVAC system performance. The predicted outputs reported as results were those produced by the Systems portion of DOE 2.1B. The energy values correspond to the loads predicted as cooling and heating coil demands. Therefore, the effect of system dynamics and thermostat set points were included.

Computations were made for two different buildings using Typical Meteorological Year (TMY) weather data for twenty cities within the United States; they were also made for a third building for five different cities. All three modeled buildings were single-story having concrete block walls and concrete slab floors.

For one of the buildings, computations were made to allow comparing the impact of two different HVAC operating schedules.

Another factor influencing the temperature of a roof's outer surface is the exterior heat transfer coefficient. The user of DOE 2.1B must specify a choice from six different correlations for the convective coefficients. For one of the buildings, comparative sets of computations were made using the available extremes of this choice.

The computed annual reduction in cooling energy needs and the annual increase in heating energy needs for each of the cases were tabulated for each location used and also graphically plotted using bar charts. The effect of roof insulation level on computations was determined and illustrated graphically for representative cases.

CONCLUSIONS:

Key conclusions of the study include:

1. Annual energy savings can be obtained via use of flat roofs with low solar absorptance, particularly with buildings at locations having large, mean, daily global solar radiation and having large cooling requirements.
2. For a flat roof having a thermal resistance of 5 ft^2-hr-F/Btu, maximum annual cooling savings were predicted for locations in the South and Southwest and were approximately 10,000 Btu/ft^2. The maximum annual heating penalties were predicted for locations in the North and in high altitudes such as Denver, Colorado, and amounted to about 4,000 Btu/ft^2.
3. Annual energy savings decreased as the roof's thermal resistance (i.e., insulation level) was increased.
4. Casting the energy savings into economic savings by assuming that heating was done by natural gas and cooling was done by an electrically driven unit indicated a maximum savings per square foot of roof surface area equivalent to the cost of about 1 Kw-hr of electrical energy.

The study helps quantify potential energy savings associated with using a flat roof having a solar absorptance of 0.3 in contrast to using one having a solar absorptance of 0.8. Further study is needed to corroborate experimentally the computer-based predictions by DOE 2.1B. Also, the effects that rain, snow, dust, and aging have on long-term performance of light-colored roofs continue to be of concern.

CHANGES IN THE HEATING AND COOLING ENERGY USE IN BUILDINGS DUE TO LOWERING THE SURFACE SOLAR ABSORPTANCE OF ROOFS

E. I. Griggs and G. E. Courville

ABSTRACT

This report addresses how changing a flat roof's solar absorptance alters the energy required to heat and cool a building. The increase in a roof's surface temperature due to insolation increases the building's heat gain during the summer and reduces its heat loss during the winter. This study examines this counteracting influence on annual HVAC energy use.

The report reviews pertinent background and presents computed changes in heating and cooling needs obtained using the computer code, DOE 2.1B. All computations were made corresponding to a reduction in a flat roof's solar absorptance from 0.8 to 0.3. They were made for two different buildings using TMY weather data for twenty cities within the United States; they were also made for a third building using weather data for five U.S. cities.

Computed annual changes in building heating and cooling energy use are presented in the form of bar charts for each location. Calculations were made for three different roof insulation levels. The change in annual energy use caused by the reduction in solar absorptance decreases with increased roof insulation. This effect is depicted graphically for representative cases.

Incorporating realistic HVAC system performance and using a particular energy cost scenario based on use of natural gas for heating and cooling via an electrically driven unit, the best cost savings occurred for locations in the Southwest and were equivalent to approximately the costs of 1 Kw-hr of electrical energy per square foot of flat roof surface.

INTRODUCTION

Sunlit building surfaces experience higher temperatures than do similar exterior surfaces not exposed to the sun. Surface temperature during sunlit hours is affected by the solar intensity, radiative characteristics of the surface, wind speed, ambient temperature, surrounding objects, and the thermal properties of the building envelope component.

Generally, solar radiation incident on the exterior surface of a building influences the loads imposed on the building's HVAC system. An increase in surface temperature due to insolation may increase the air-conditioning load during the summer or reduce the heating load during the winter. Since these are counteracting influences, questions arise as to how annual HVAC energy requirements are changed when a surface's radiative properties are altered. If the solar absorptance of a sunlit surface is lowered, the cooling load and heating load, associated with solar incidence, will be lowered and raised, respectively. Should changing the solar absorptance result also in a change in the infrared emittance, loads will also be affected by the altered infrared radiative exchange with the surroundings.

This study focused specifically on how reducing the solar absorptance of a roof's surface affects annual heating and cooling loads. The effort was undertaken in conjunction with a program on roofing research being conducted at the Oak Ridge National Laboratory (ORNL). The energy-saving potential associated with roof construction and the need for further research has been established and reported elsewhere [1, 2]. The possibility of conserving energy by using reflective materials for the outermost roof layer represents one area of interest. The computer code, DOE 2.1B, was used to calculate HVAC load changes resulting from a change in the solar absorptance of a roof's surface. Prior to presentation and discussion of results, some relevant background is outlined in Sections 2 and 3.

2. LITERATURE REVIEW

Attention is given in this chapter to literature that deals with how solar absorptance affects roof surface temperature and the net energy transfer through a roof. In practice, quantification of these effects is dependent on reliable solar absorptance values for the materials of interest. Reported solar absorptance values for building materials are discussed first.

2.1 REPORTED SOLAR ABSORPTANCE VALUES

In discussing roof design with respect to energy conservation, Probert and Thirst [3] noted that summer heat gain can be reduced by judicious selection of roof color. Solar absorptances values given in their paper are listed in Table A.1 of Appendix A. Values range from 0.45 for a "white" surface to 0.95 for a "black" surface. Table A.2 lists some solar absorptances which are given by Baker [4]. There is good agreement between the values in Table A.1 and Table A.2.

Reagan and Acklam [5] have also reported solar reflectances of several types of building materials. They stated that solar absorptance and reflectance data for common building materials were rather sparse; consequently, they developed a probe for measuring solar reflectance in their study. The effective spectral range of their probe was stated to be 0.44 to 0.96 microns. Noting that this range did not encompass the total solar spectrum, they reasoned that the solar reflectance of coatings commonly used in buildings does not deviate significantly in the 0.96 to 2.0 micron range from that exhibited in the visible wavelength range. Reflectance measurements were made on a variety of wall and roofing materials. Reflectance values given in this paper are listed in Tables A.3 through A.7. Of particular interest in this work are the values given in Table A.7 for coated and built-up roofs. For listed materials the absorptance ranges from 0.25 and 0.88. Based on their measurements, they proposed a color classification scheme for calculating building heat gains and losses. The classification scheme with the corresponding values for reflectance and absorptance is given in Table A.8.

In a document related to energy savings, Talbert [6] reports values of solar reflectance and thermal emittance for several types of roof surfaces. These were reported as being measured by the DSET Laboratories of Phoenix, Arizona. Listed in Table A.9 are their reported reflectance values along with absorptance values calculated for an opaque surface.

The user of DOE 2 has the option of specifying the solar absorptance of exterior surfaces for the building being modeled. A list of solar absorptance values is given in the DOE 2.1B Reference Manual [7]. This list is included in Table A.10 for reference.

2.2 SURFACE TEMPERATURE

Exposure of a roof membrane to large temperature swings may lead to a reduction in its useful life as a consequence of numerous problems resulting from the cycling stressing such as cracking. Surface color and the amount of insulation between the membrane and the deck affect membrane temperature. Rossiter and Mathey [8] calculated steady-state surface temperatures of black (α = 0.9), gray (α = 0.7) and white (α = 0.5) roofs for various thicknesses (zero to five inches) of insulation located between the membrane and roof deck. While focusing principally on the influence of added insulation, their results also illustrate the influence of the roof's solar absorptance. Their results indicated that the first increment, about one inch, of insulation causes a significant rise in the roof surface temperature due to solar radiation, but additional increases in thickness above this first increment does not appreciably increase the roof surface temperature. The color distinction had a more marked effect on predicted roof temperature than did the amount of insulation placed beneath the roof membrane.

In a study of two contiguous buildings, Shuman [9] made comparisons of heat flow through wet and dry insulated roof constructions and also made measurements for some thermal effects associated with three different roofing granules. Roof coverings included slag, white marble containing dark constituents of about 15 percent and slag coated with an experimental water-paint of white portland cement with plasticizer. Shuman concluded that roof reflectance should be considered in design. He emphasized need for reliable reflectance data and the importance of an acceptable service life.

Baker [4] stated that temperatures which roofing materials experience during their service life may well determine the success or failure of a roof system. He reports that the surface temperature of a roof may reach 88°C (190°F) for a flat roof having an unobstructed view of the sky. Some simple formulae for estimating roof temperature during both day and night operation are given in his book.

Keeton and Alumbaugh [10] experimentally investigated the effects of insulation upon temperatures within built-up roofs. Three temperaturecontrolled buildings were built to accommodate testing of 8-ft-by-8-ft built-up roofs. Their tests incorporated surfacings classified as white, white gravel, gray gravel, aluminum gray and black. One of their recommendations was that serious consideration should be given to changing the surfacing of a roof to a lighter color as an alternative to more expensive reroofing when it is necessary to improve thermal resistance of an existing roof to lower energy consumption.

The publications just reviewed imply that reflective roofs operate cooler than comparable ones having a larger solar absorptance. Improved roof-membrane life and energy conservation may both be desirable consequences of reduced surface temperature.

2.3 ENERGY USE CONSIDERATIONS

Since the heat transfer through a building envelope component, such as a roof, depends on surface temperatures, the influence of solar absorptance on sunlit surface temperatures may alter heat transfer rates. In contemporary methods for estimating air-conditioning cooling loads, such as the procedure outlined in the 1981 ASHRAE Handbook of Fundamentals [11], calculations of loads depends on specification of the color of exterior wall and roof surfaces. Color consideration is typically discussed only in connection with cooling loads since traditional load calculation schemes are to determine the maximum for purposes of sizing equipment. The maximum cooling load will include solar contribution; however, the maximum heating load will occur in the absence of solar exposure. As attention is directed more specifically to energy utilization, the impact of solar influences on both heating and cooling energy use needs to be evaluated.

The simplest approach to estimating energy requirements is to use steady-state calculations and to relate requirements to net instantaneous rates of heat transfer. This scheme, however, fails to incorporate many important factors. Such features as structural energy storage, thermostat set points, HVAC equipment operating characteristics, the distinction between instantaneous heat transfer rates and coil loads, the coupling between internal loads and external loads and other interrelated effects serve to make the calculation of actual energy requirements a more formidable problem than that of making simple steady-state calculations.

Recent attention has been given to the role that roof "color" has in altering energy requirements for the heating and cooling of buildings. In an extensive treatise on energy conservation, Dubin [12] presented nomographs for the heat gains and losses for roofs. These nomographs facilitate estimation of the effect of changing the solar absorptance from 0.8 to 0.3 on both heat gain and heat loss.

In an assessment of the energy-saving potential of roofing research within the United States, Chang and Busching [2] used Dubin's nomographs to estimate heat gains and losses for numerous locations. They noted that the annual heat loss through a roof with a surface absorptance of 0.8 is approximately 12 to 25 percent less than the annual heat loss through a similar roof with a surface absorptance of 0.3 and that the annual heat gain for $\alpha = 0.8$ is approximately two to four times that for $\alpha = 0.3$. Surface solar absorptance of a low-slope roof was concluded to be an important factor affecting heat loss and gain.

The influence of surface solar absorptance on heat transfer through opaque building elements was also addressed by Reagan and Acklam [5]. They discussed results of heat gain/loss calculations made for several residences in Tucson, Arizona. Comparative results for daily average heat gain were given for one residence; values of α for the roof of 0.75 and 0.35 were used. One case corresponded to a poorly insulated home; the other case was for a more modern, better insulated home. They concluded that changing the roof color from dark to light does greatly reduce the roof heat gain of a typical southwestern house during the summer, but such a reduction has little effect on the summer total-house heat gain because the roof's contribution is only a small part of the total.

Griffin [13] outlined a scheme for estimating cooling-energy cost savings with the use of heat-reflective, aluminum asbestos-fibrated coatings, instead of conventional black asbestos-fibrated coatings, on smooth-surfaced built-up bituminous membranes. His estimation scheme was based on use of the total equivalent Cooling Load Temperature Difference (CLTD) as described in the 1981 ASHRAE Handbook of Fundamentals [11]. Tabulated CLTD values were corrected by a color adjustment factor. For climates with long cooling seasons, Griffin reported that a savings of $0.25/ft^2 in present worth can be achieved over 20 years; it was, however, noted that other climatic conditions tend to complicate the impact of changing α on heating energy consumption.

Talbert [6] summarized a brief study that focused on potential energy savings with buildings whose roofs are coated with aluminum flakes exhibiting high solar reflectance and low thermal emittance. The report includes estimated cooling energy savings that might be realized in Phoenix, Arizona, by use of the aluminum flakes. Estimates were made by two methods. The first was based on the scheme reported by Griffin [13]. The second was based on use of an average daily sol-air temperature and steady-state calculation. Noting that the methods were developed to determine design loads for equipment sizing, Talbert cautioned that predicted energy savings may not be very accurate. He suggested that a better method would be to utilize one of the more sophisticated computer models. Specific reference was made to DOE 2.

2.4 SUMMARY

The preceding literature review reveals current interest in studying the thermal effects related to solar reflective and absorptive characteristics of roof surfaces. Lower roof absorptance results in lower surface temperatures during sunlit hours. Lower surface temperature can alter both cooling and heating energy requirements. The net effect is dependent upon several weather-related factors. Allusion to the need for use of sophisticated computer programs to more accurately estimate energy savings has been made and seemed to be a logical next step.

3. RELATED CONCEPTS

Certain concepts fundamental to this study are discussed in this section. Thermal radiation, concept of sol-air temperature and the apparent effect on building energy loads caused by changing the solar absorptance of the roof's surface are briefly outlined.

3.1 THERMAL RADIATION CONSIDERATIONS

This work focused on how changing the solar absorptance of a flat roof's exterior surface affects heat transfer through the roof.

Often the radiative characteristic of a surface is discussed in terms of color. Generally color relates to the visible portion (0.35-0.7 μ) of the electromagnetic spectrum; hence, color may not always convey an accurate description for the complete thermal-radiation band. Radiative heat transfer between objects at low temperatures involves long-wavelength (> 8μ) radiation. The energy transmitted as solar radiation is concentrated in a band of shorter wavelengths. For example, modeling the sun as a blackbody emitter at 6000 K, 99.5 percent of the emitted energy lies between 0.1 and 5 microns and 43.2 percent lies in the visible spectrum (0.35 to 0.7 μ).

When a material layer is exposed to radiant energy, a portion is reflected, a portion may be transmitted and the remainder is absorbed. An energy accounting for radiant energy of any wavelength leads to

$$\alpha_\lambda + \rho_\lambda + \tau_\lambda = 1 \qquad (3.1)$$

In general, radiative properties of materials are directional and spectrally dependent; however, many engineering analyses are made using hemispherical values. Also, for most engineering applications, material layers are opaque which means that none of the incident radiant energy is transmitted through the layer (i.e., $\tau = 0$). The absorption and reflection processes are treated as surface phenomena.

In terms of hemispherical properties, the accounting of radiant energy impinging upon an opaque layer is given by

$$\alpha + \rho = 1 \tag{3.2}$$

According to Kirchhoff's law, absorptance equals emittance under conditions of thermal equilibrium, but this equality is often assumed in engineering analyses of non-equilibrium situations. When this is done, $\alpha = \varepsilon$ and Equation (3.2) becomes

$$\varepsilon = 1 - \rho \tag{3.3}$$

Kirchhoff's law is not necessarily true for all real situations. For example, one area of research on improving solar collector performance has focused on materials having an α/ε ratio greater than unity. For common roofing materials, data relating α and ε seem to be lacking.

3.2 SOL-AIR TEMPERATURE

The net heat transfer from the sun and other exterior surroundings to a roof's surface involves absorption of solar energy, convective exchange with the environment and an infrared radiative exchange with low-temperature surroundings. The sol-air temperature is defined as the "hypothetical" air temperature that would result in the same net heat transfer to the surface using a combined radiative and convective heat transfer coefficient. Using the definition, the sol-air temperature can be written as

$$T_{sa} = T_\infty + \frac{\alpha G}{h_o} - \frac{\varepsilon \Delta E}{h_o} \tag{3.4}$$

In Equation (3.4) T_∞ denotes the outside air temperature, α denotes the surface's solar absorptance, G denotes the incident solar flux, ε denotes the surface's infrared emittance, ΔE denotes the difference between the energy emitted by a blackbody at T_∞ and the longwave radiation incident on the surface, and h_o denotes the combined convective and radiative coefficient. The combined coefficient h_o is expressed by

$$h_o = h_e + h_r \tag{3.5}$$

where

$$h_r = \varepsilon\sigma(T_0^2 + T_\infty^2)(T_0 + T_\infty) \qquad (3.6)$$

Both h_e and h_r are temperature dependent, and h_e depends on the air flow pattern near the surface. While sol-air temperature is useful for illustrating the effect of solar loading, it is not an independent property of the climate because of its dependence on the parameters α, ε, h_0, and ΔE. The definition of sol-air temperature is used in the discussion which follows.

3.3 DISCUSSION OF CHANGES IN BUILDING LOADS DUE TO CHANGE IN THE SOLAR ABSORPTANCE OF THE ROOF

This discussion focuses on how a discrete change in a roof's solar absorptance (α) alters heating and cooling loads.

3.3.1 Definition and Illustration of Terms

If α of a roof's surface is lowered, the energy required for cooling the contiguous building will most likely be reduced because the cooling loads will be smaller following the reduction in surface temperature during sunlit hours. High roof surface temperatures during the winter may tend to impede heat loss through the roof. Hence, using a reduced surface α during the winter may likely result in an increase in the energy requirements for heating.

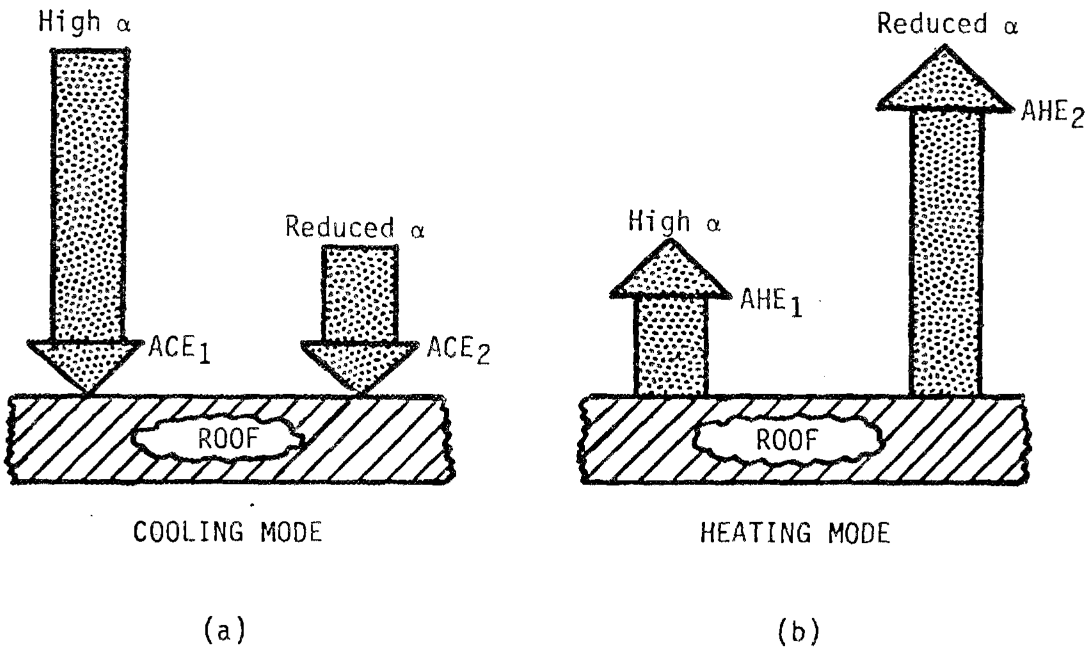

Figure 3.1 Illustration of Load Change Due to Discrete Change in Roof's α

Figure 3.1(a) illustrates the possibility of reducing annual cooling energy per unit roof area (ACE) by lowering the roof's α. Similarly, Figure 3.1(b) shows the converse for the possibility of increasing annual heating energy per unit roof area (AHE) by lowering α of the roof. A principal goal of this study was to assess changes in ACE and AHE due to a discrete reduction in α. For this purpose ACES denotes the magnitude of annual cooling energy saving, and AHEP denotes the magnitude of annual heating energy penalty, both based on unit roof area. With reference to Figure 3.1, ACES and AHEP are expressed by

$$ACES = ACE_1 - ACE_2 \qquad (3.7)$$

$$AHEP = AHE_2 - AHE_1 \qquad (3.8)$$

Both ACES and AHEP represent changes in annual energy requirements due to a lowering of a roof's α. Both are defined in the positive sense.

3.3.2 Steady-State Calculation of Roof Heat Transfer Using Sol-Air Temperature

A steady-state calculation of roof heat transfer may afford insight into how changing α affects energy use. Consider a unit area of roof over a conditioned space, which for the purpose of this evaluation, is to be maintained at a constant temperature T_i. Using sol-air temperature, the net annual heat gain through the roof per unit area is given by

$$\text{Net Annual Gain per Unit Roof Area} = \int U_o(T_{sa} - T_i)dt \qquad (3.9)$$

where U_o represents the overall heat transfer coefficient for heat transfer between air at the sol-air temperature and that inside at T_i. The integral is to be evaluated over one year. Specific separation of the net gain into ACE and AHE requires more detailed insight into hour by hour building operation. For example, heat gain through the roof may contribute to a cooling load or may reduce a heating load, depending on which mode prevails within the space at that time.

The definition of sol-air temperature given in Equation (3.4) can be used in Equation (3.9). The net gain can then be evaluated for a large value of α and also for a lower value of α. The difference obtained by subtracting the net gain for the lower α from that corresponding to the higher α, assuming that ϵ, h_o and ΔE are unaffected by the changed α, is given by

$$\text{Net Annual Reduction in Heat Gain} = \int \frac{\Delta\alpha\ U_o\ G}{h_o}\, dt \qquad (3.10)$$

Since the net reduction in energy gain is partially a saving in cooling energy (ACES) and partially a penalty in heating energy (AHEP), the left side of Equation (3.10) actually represents the sum ACES + AHEP. If a particular location is characterized by essentially no annual heating requirement, such as southern Florida, then the net reduction in heat gain is almost totally ACES. Conversely, should a particular location be characterized by essentially no cooling requirements, then the net reduction in heat gain would be almost totally AHEP.

If U_o and h_o are assumed constant, the steady-state value given by Equation (3.10) for a flat roof is

$$\text{ACES} + \text{AHEP} = \left(\frac{\Delta\alpha U_o}{h_o}\right)(365\ \bar{G}_{S_D}) \qquad (3.11)$$

where $\bar{G}_{S_D}$ represents the average daily solar flux on a horizontal surface. Subject to the limitations in going from Equation (3.10) to Equation (3.11), it can be noted that the net reduction in energy gain (ACES + AHEP), due to a reduction in a roof's solar absorptance by the amount $\Delta\alpha$, varies linearly with $\bar{G}_{S_D}$. Also, with other parameters unchanged, an increase in h_o causes a decrease in the sum (ACES + AHEP), an observation that illustrates the important role of the factors which control h_o such as wind velocity. Equation (3.11) was used in this study to determine steady-state estimates for (ACES + AHEP) against which nonsteady-state (ACES + AHEP) values obtained using DOE 2.1B for actual buildings were compared.

Division of the net reduction into separate values for ACES and AHEP for a real building operating in a location having both significant heating and cooling loads is dependent on local climate, building type and HVAC operation. Figure 3.2 portrays four situations to illustrate qualitatively the possible relationships between inside temperature T_i and sol-air temperature for two different α values. The sol-air curves were drawn using sol-air temperatures given in the 1981 ASHRAE Handbook of Fundamentals [11] for a particular location. Here, however, the curves are intended only for qualitative comparison. For some days, sol-air temperatures for both values of α may totally lie below T_i. Conversely, for some days, they may be totally above T_i. Both may cross T_i for some days and for some only the curve for high α may cross T_i. The point here is that the temperature difference between sol-air temperature and inside temperature and how this difference is altered by changing α is definitely dependent on the local climate since the sol-air temperature is affected by climatic variables as shown by Equation (3.4).

Results for ACES and AHEP which were determined for several cases using DOE 2.1B are presented and discussed in the next section.

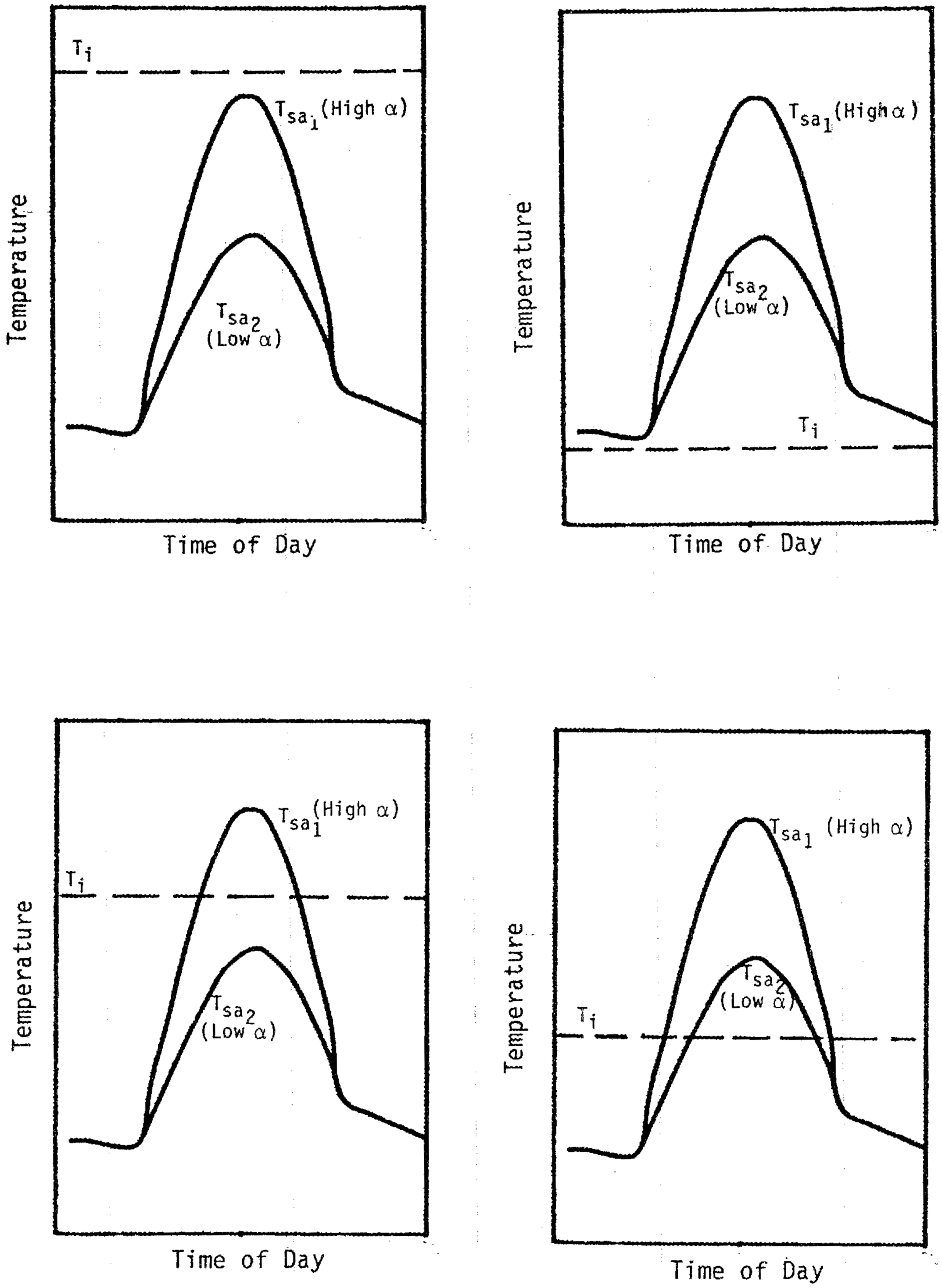

Figure 3.2 Illustration of Possible Sol-Air Temperature Variation in Relationship to Inside Temperature

4. PRESENTATION AND DISCUSSION OF RESULTS

4.1. INTRODUCTION

The object of this this work was to calculate changes in heating and cooling energy requirements for a building when the solar absorptance (α) of its roof's surface is changed. All computations correspond to a reduction in α from 0.8 to 0.3. The study focused on two single-story buildings having concrete block walls and concrete slab floors; a few computations were also made for a third building similar to the other two except for more zoning used with the HVAC system. Twenty locations were used for many of the calculations; however, some calculations were made for only fifteen locations. Prior to presentation of calculated results in this section, the utilized computer code, DOE 2.1B, is briefly discussed. Also discussed are some special considerations pertinent to the work.

4.2 DOE 2.1B

DOE 2.1B is a computer code widely used for modeling buildings and their associated heating and cooling systems. It is a versatile code which can simulate hour-by-hour performance of a building throughout a year.

DOE 2.1B consists of numerous subprograms, two of which are the LOADS program and the SYSTEMS program. In the LOADS program, hourly heat gains and losses through the building envelope components are first calculated separately. Weighting factors are then used to convert gains into loads. In the calculation of heat gains and losses through exterior walls and roofs, the effect of thermal storage can be taken into account through the use of thermal response factors. All computations in LOADS are made on the basis of a fixed temperature for conditioned spaces. The SYSTEMS program uses the output of the LOADS program, HVAC system characteristics, and room air weighting factors to determine the hourly energy requirements imposed on the HVAC system. In this process, the SYSTEMS program modifies the loads to account for variable temperatures in each conditioned zone.

The flexibility of DOE 2.1B affords opportunity for comparing computed energy values corresponding to a rather wide range of options in the modeling. For example, the output of LOADS corresponds only to a fixed space temperature. On the other hand, the output of SYSTEMS (e.g., coil loads) takes into account different thermostat setpoints for heating and cooling, scheduling of HVAC operation, scheduling of various internal loading and HVAC equipment specifications. If the HVAC system capacity is not specified, DOE 2.1B sizes the equipment automatically from loads determined in the LOADS program. Thus, if a building-envelope parameter is changed between two runs, the change in computed loads may lead to a different size HVAC system for the second case than was determined for the first case. The user, however, has the option of inputing HVAC equipment capacity. Comparisons of building energy use between two runs where the HVAC equipment has been sized automatically would seem more appropriate for examining the effect of changing a building-envelope parameter in design considerations of new buildings. Conversely, the effect of changing the building-envelope parameter for an existing building for which the same HVAC equipment is to be used before and after the change would seem best determined by specifying the same equipment capacities for both runs.

Some preliminary computer runs were made using only the LOADS subprogram. Output of LOADS corresponds to a fixed space temperature being maintained around the clock. The principal focus of the study, however, was directed toward total building simulation which included effects of scheduling and HVAC system operation. Attention was focused on the calculated changes in annual heating coil load and annual cooling coil load which was output by the SYSTEMS subprogram.

4.3 SPECIAL CONSIDERATIONS FOR THIS STUDY

4.3.1 Weather Data

DOE 2.1B is designed to receive climate-related variables from weather tapes. For this study Typical Meteorological Year (TMY) weather tapes were used. Thirty locations were used for most of the preliminary (LOADS) computer runs. Twenty of these locations were used for several computer runs where attention was focused on the output of the SYSTEMS subprogram; however, some cases were examined for only fifteen locations. Although selected partially on the basis of available TMY weather tapes which had been configured for DOE 2.1B input, the locations were chosen to represent the range of heating and cooling requirements within the United States. Figure 4.1 shows cooling-degree days versus heating-degree days for over two hundred weather-reporting stations within the United States. Data for the plot was taken from Reference 14. The twenty selected locations, indicated by the heavier darkened circles, are dispersed throughout the range of conditions represented by the data of Reference 14. Table 4.1 lists these twenty locations together with values for the cooling-degree days, heating-degree days, average daily solar flux, and average wind speed. The average wind speed was obtained from Reference 15.

4.3.2 Values of Solar Absorptance

Values of 0.8 and 0.3 were used for the roof's solar absorptance. These values represent practical bounds of absorptance. This can be seen by inspection of the reported values listed in Appendix A. These two values were also used in the work of Dubin and Long [12] and that of Chang and Busching [2].

4.3.3 Overall Heat Transfer Coefficient

With load-calculating methods such as those outlined in the ASHRAE Handbook [11], air-film coefficients on the inside and outside of a roof, h_i and h_e respectively, are included with the roof

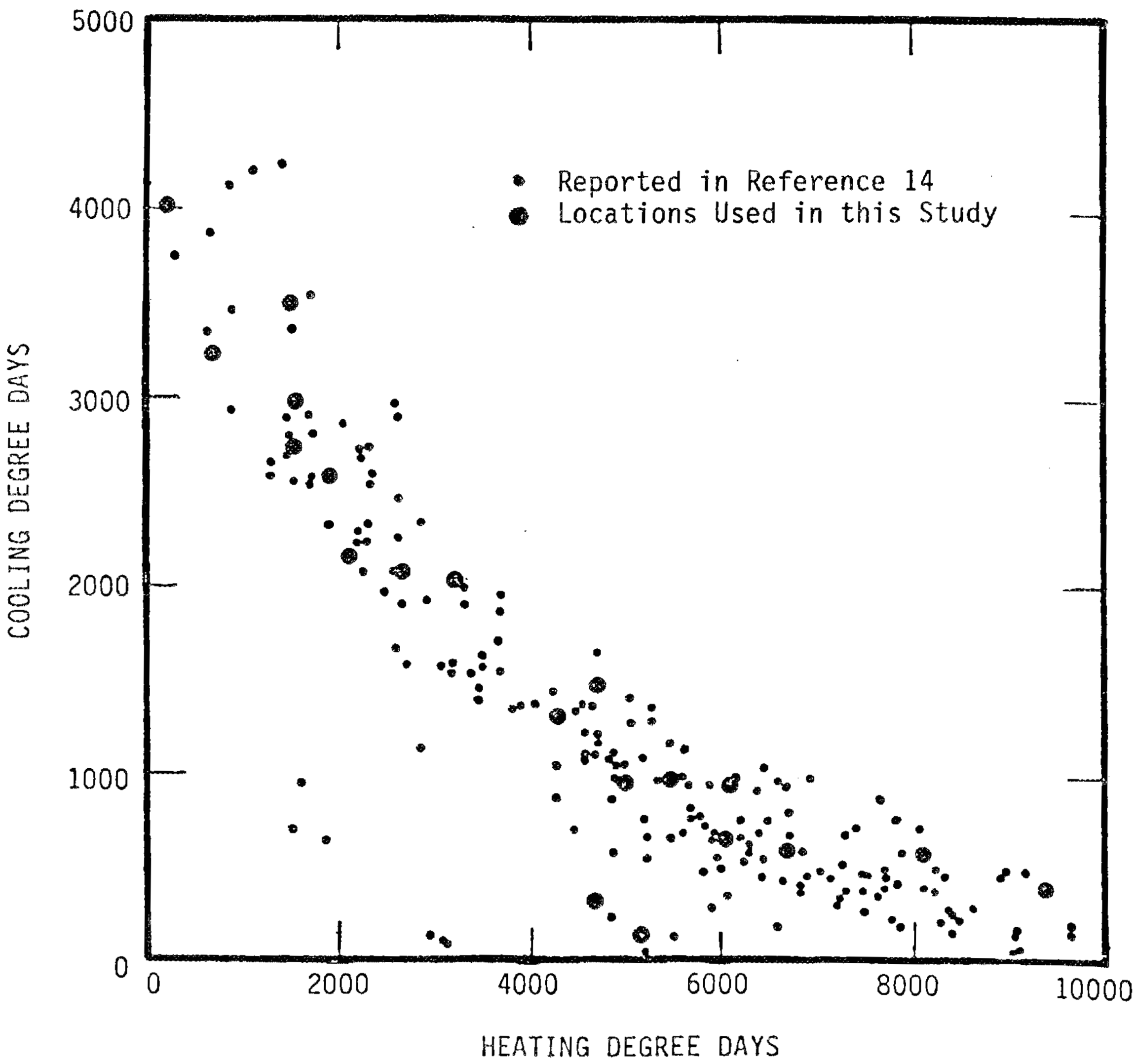

Figure 4.1 Cooling Degree Day and Heating Degree Day Data for Over Two Hundred Weather Reporting Stations in the United States

Table 4.1 Climate-Related Data for Twenty Locations Used in this Study (Sources: References 14 and 15)

Location	CDD	HDD	$\overline{G}_{S_D}$ (Btu/day·ft²)	$\overline{V}$ (mph)
Phoenix, AZ	3506	1552	1869.4	5.1
Bakersfield, CA	2178	2183	1749.2	6.9
El Paso, TX	2097	2677	1899.7	8.1
Albuquerque, NM	1316	4291	1827.5	9.4
Miami, FL	4037	205	1472.9	9.4
San Antonio, TX	2993	1570	1499.0	9.4
Tampa, FL	3366	716	1492.1	8.3
Augusta, GA	1994	2547	1361.6	6.7
Lake Charles, LA	1738	1498	1364.6	8.7
Memphis, TN	2029	3226	1365.9	8.9
Denver, CO	625	6016	1568.4	11.2
St. Louis, MO	1474	4748	1326.6	9.6
Washington, DC	940	5009	1208.4	7.8
Chicago, IL	923	6125	1215.1	10.7
Indianapolis, IN	974	5576	1165.0	8.9
Minneapolis, MN	585	8158	1170.2	10.1
Minot, ND	369	9407	1178.3	10.3
Syracuse, NY	551	6678	1034.5	10.1
Portland, OR	299	4792	1066.8	8.3
Seattle, WA	128	5184	1052.7	8.7

resistance, R, in determining the overall thermal conductance, U. The expression is

$$U = \frac{1}{1/h_i + R + 1/h_e} = \frac{1}{1/U' + 1/h_e} \quad (4.1)$$

The coefficient U given by Equation 4.1 represents the traditionally computed value to be used for calculating steady-state heat transfer when using outside air-to-inside air temperature difference. The definition of sol-air temperature given earlier incorporates the radiative energy exchange occurring at exterior surfaces. A combined convective and radiative coefficient, h_o, is defined for exterior surfaces and is used to compute U_o, which represents the coefficient to use for calculating steady-state heat transfer using sol-air-to-inside-air temperature difference. In this context

$$U_o = \frac{1}{1/U' + 1/h_o} \quad (4.2)$$

The quantities R and h_i, thus U', remain constant during a particular DOE 2.1B run while the external combined resistance ($1/h_o$) varies with external environmental conditions.

The DOE 2.1B algorithm for an energy balance at the outer surface of a roof involves h_o which is the combined convective and radiative coefficient. Since the external coefficient h_o varies with time, the constant U' values are used hereafter to characterize the roof's relative insulation level. This is done since U' is a constant throughout a computer run while U and U_o vary slightly hour by hour due to the dependence of h_e and h_o on wind speed. Options are provided for the user of DOE 2.1B to choose several functional relationships relating h_o to wind speed. Distinction between correlations is related to roof roughness. These correlations of h_o with wind speed are listed and graphed in Appendix C.

4.4 RESULTS OF CALCULATIONS USING ONLY THE LOADS PROGRAM

The LOADS subprogram of DOE 2.1B was used to make a series of calculations. These preliminary calculations were made to gain insight into the effects of location, roof insulation level and roof insulation type and to help reduce the number of computer runs required for the more complete building simulations where system effects were included. Results of the preliminary calculations are included for reference in Appendix D.

4.5 BUILDING SIMULATIONS

Three different single-story, concrete-slab-floor buildings, designated hereafter as Buildings A, B, and C, were considered in this study. The flat-roof construction was specified to be the same for all three buildings. Buildings A and B involved only one interior zone, and Building C involved five interior zones. Building A had a suspended ceiling between the roof and the conditioned space, and the return air was directed through the unconditioned space between the ceiling and roof. The inner surface of the roof for Building B and Building C was directly contiguous to the conditioned space. Building A was described to model a typical interior office module with a strip of contiguous identical units. Building B was specified to model an open-area repair shop or light manufacturing facility. Building C represented a multizone office building. More complete descriptions of the three buildings are given in Appendix E.

4.5.1 Building A

Using Typical Meteorological Year (TMY) weather data for twenty locations, Building A was first examined for the case of a roof U' value of 0.2 Btu/hr-ft^2-F. As discussed earlier, U' is based on the combined resistance of the roof materials and the inside convective air-film resistance. For the roof construction considered, a U' value of 0.2 Btu/hr-ft^2-F corresponds to an insulation thickness yielding an R value of 3.74 hr-ft^2-F/Btu. The remainder of the resistance, 1.26 hr-ft^2-F/Btu, is due to the aggregate, built-up roof membrane, steel deck and interior air-film. For other U' values, the contribution due to aggregate, built-up roof membrane, steel deck and interior air-film remained constant. The quoted U' value was obtained by changing only the thickness of insulation. For two larger thicknesses of insulation, runs were made for fifteen of the selected locations. DOE 2.1B was allowed to size the equipment automatically for all Building A runs. Changes in predicted cooling coil load, heating coil load, electrical energy required by the system fan and the electrical energy required by the cooling system are tabulated in Appendix F, Tables F.1 through F.3. For the lowest level of insulation considered (U' = 0.2 Btu/hr-ft^2-F), changes in predicted HVAC coil loads are depicted by the bar graph of Figure 4.2. The results have been arranged by descending values of the net effect (ACES + AHEP). Noting values listed in Table 4.1 of the daily mean global solar radiation $\bar{G}_{S_D}$ on a horizontal surface for each of the locations, it is noted that (ACES + AHEP) generally increases with an increase in $\bar{G}_{S_D}$. See Figure 4.3. For the Building A cases examined, each predicted ACES value is larger than the corresponding AHEP value indicating that predicted energy savings during cooling exceeds the energy-use penalty during heating. Economic savings depend, however, on the type of cooling and heating systems used and on the relative costs of heating and cooling energy. This practical concern is discussed later in more detail.

The sum (ACES + AHEP) decreases with an increase in the R-value of roof insulation. This is shown in Figure 4.4 for four locations selected to show the range of computed values. Figure 4.4(a) shows that the net reduction in energy gain, as realized at the coils, due to changing the roof's surface solar absorptance decreases with an increase in the thermal resistance. Figure 4.4(b) shows the excess

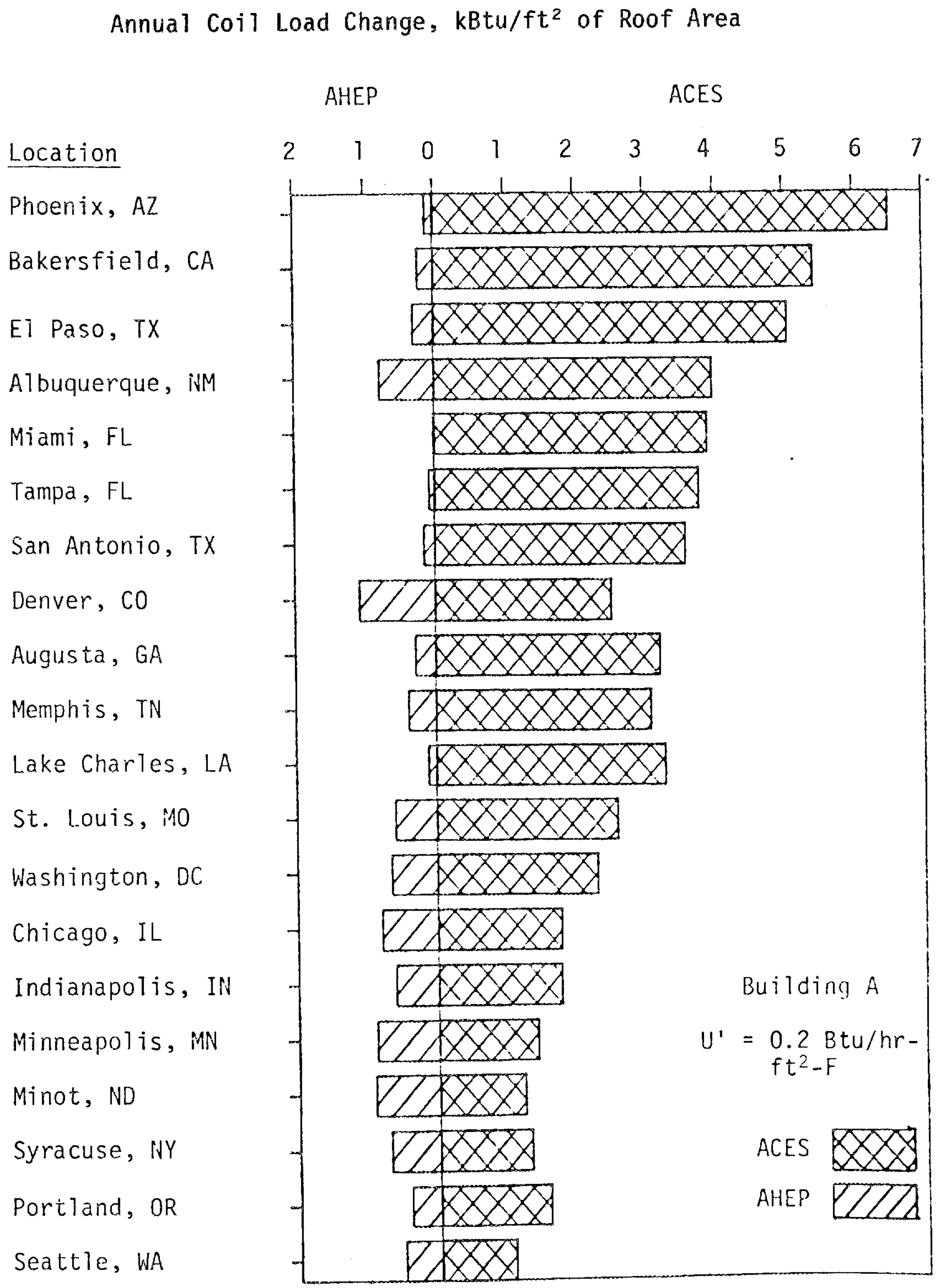

Figure 4.2 Comparison of HVAC Coil Load Changes (ACES and AHEP) Predicted by DOE 2.1B Systems for Building A Due to a Lowering of the Roof's Solar Absorptance from 0.8 to 0.3

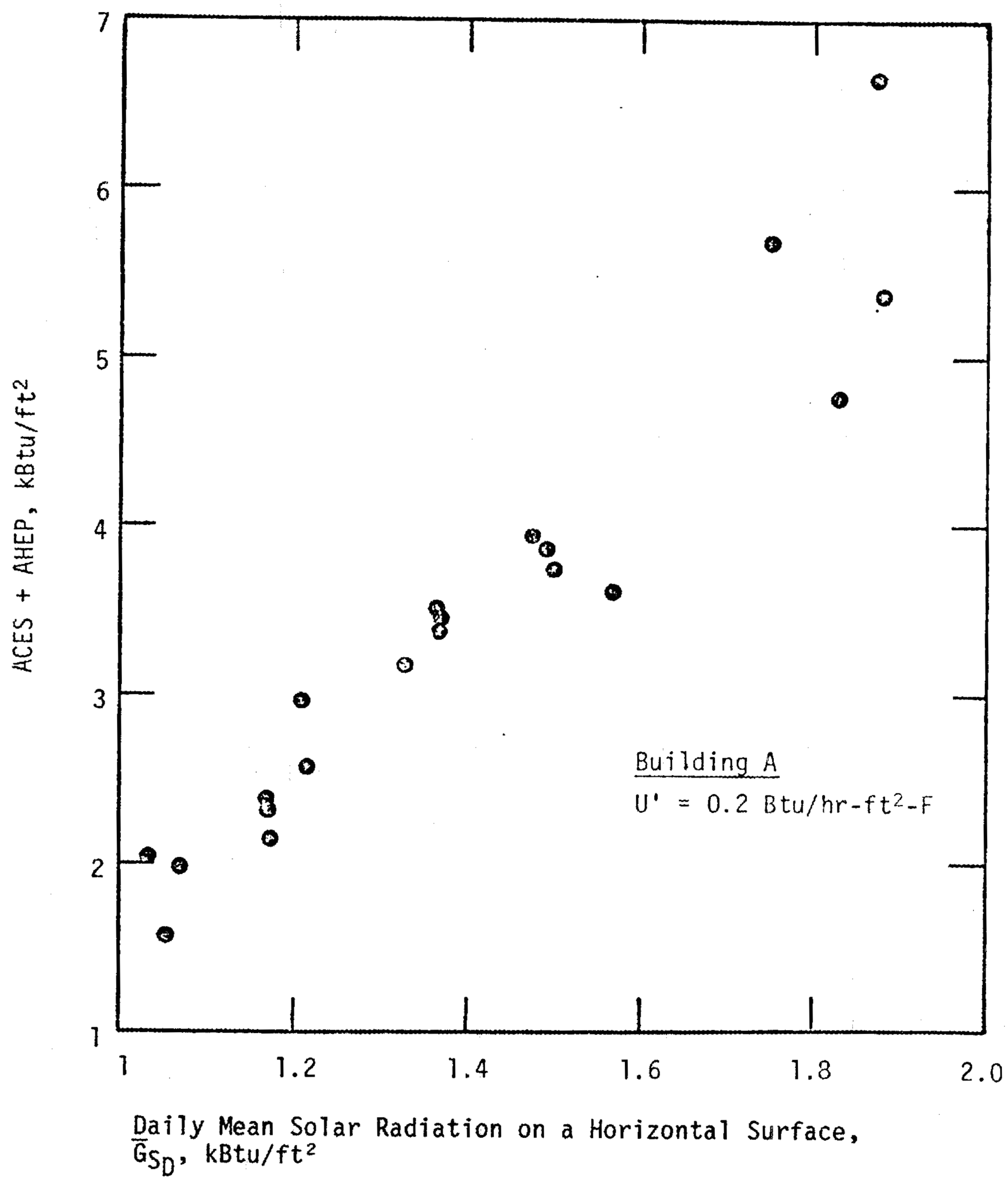

Figure 4.3 Illustration of Variation of (ACES + AHEP) with the Daily Mean Solar Radiation on a Horizontal Surface (Building A; $U' = 0.2$ Btu/hr-ft^2-F)

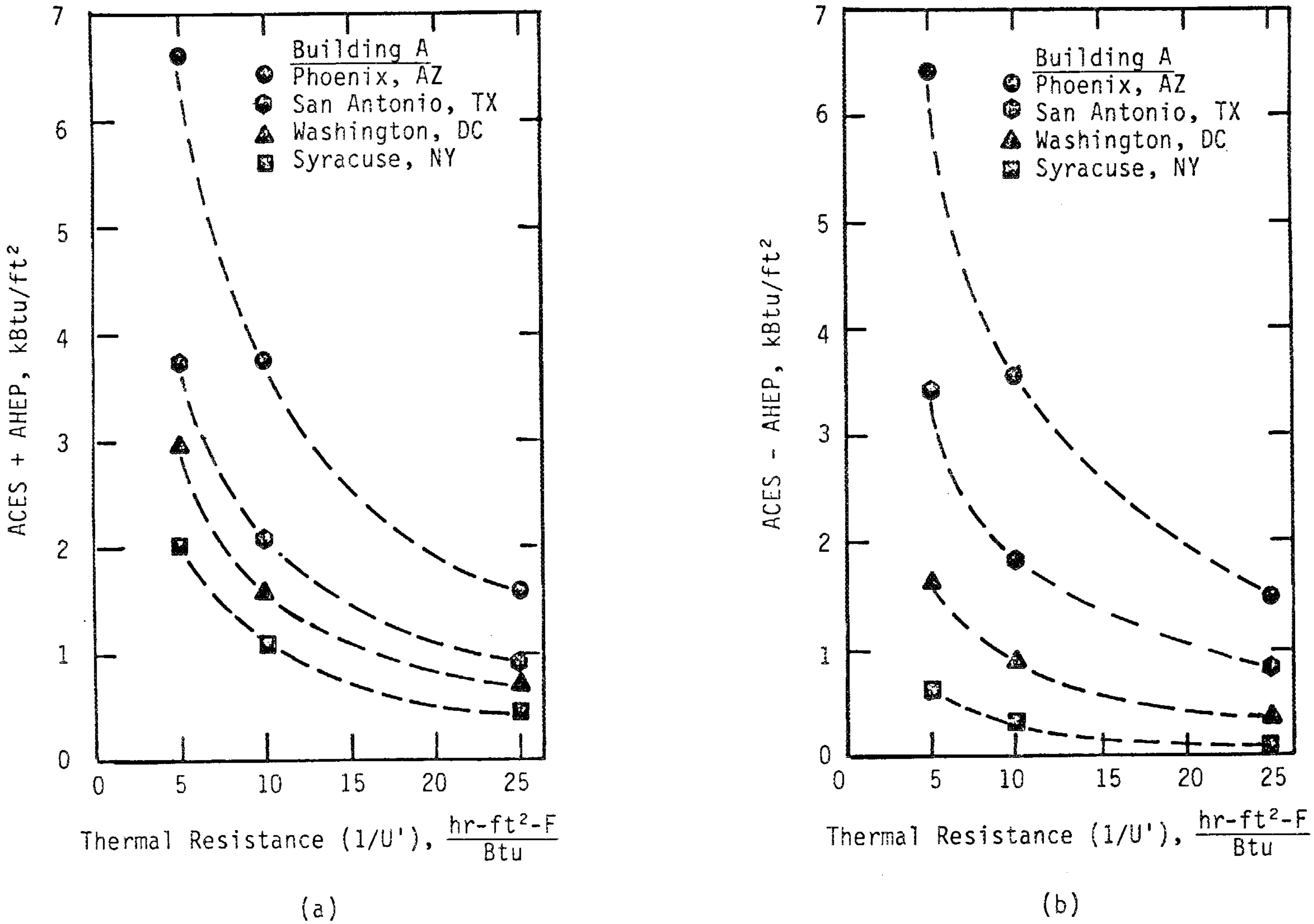

Figure 4.4 Illustration of the Effect of Thermal Resistance on Computed (ACES + AHEP) and the Difference (ACES - AHEP) for Building A

of cooling energy savings over heating energy penalty for the same four locations. Similar behavior occurred for all locations examined. This can be seen by inspection of the computational results listed in Tables F.1 through F.3.

4.5.2 Building B

Building B was examined for several cases, hereafter referred to as Cases B1, B2, B3, and B4. Case B1 involved operating conditions similar to those used for Building A. Nighttime and weekend setback of thermostats was used and DOE 2.1B was again allowed to automatically size the HVAC system on the basis of loads computed in the LOADS subprogram. For fifteen locations and three different insulation levels, predicted changes in cooling coil load, heating coil load, electrical energy required by the system fan the the electrical energy required by the cooling system are tabulated in Appendix F, Tables F.4 through F.6. Figure 4.5 shows predicted changes in HVAC coil loads for Case B1 and an insulation level yielding a U' value of 0.2 Btu/hr-ft^2-F. Results for Case B1 exhibit trends similar to those for Building A. The net reduction in energy gain (ACES + AHEP) increases nearly linearly with the average daily solar radiation $\bar{G}_{SD}$. This is shown in Figure 4.6. The decrease of the sum (ACES + AHEP) with an increase in the R-value of roof insulation is depicted in Figure 4.7 for the same four locations used in illustrating the trend for Building A. Figure 4.7(a) shows how the net effect varies with roof thermal resistance for the four selected locations. Figure 4.7(b) illustrates how the difference (ACES - AHEP) varies with the thermal resistance. The behavior is similar for all fifteen locations that were examined; results are listed in Tables F.4 through F.6. Since results for Building A and for Case B1 of Building B illustrated similar dependence of predictions on insulation level, only a U' of 0.2 Btu/hr-ft^2-F was used for subsequent runs (Cases B2, B3, B4) where the effect of other parameters was examined.

Case B2 designates another set of calculations for Building B where nighttime and weekend setback of thermostats was again used but the HVAC system capacity was forced to be the same for the α = 0.3 case as that generated by DOE 2.1B for the α = 0.8 case. For fifteen locations, predicted changes in cooling coil load, heating coil load, electrical energy required by the system fan and the electrical energy required by the cooling system are tabulated in Appendix F, Table F.7. The coil load increments, ACES and AHEP, are depicted in Figure 4.8 where also the results for Case B1 are repeated to accommodate comparison between Cases B1 and B2. The comparison shows that forcing the system capacity to be the same for both values of roof absorptance (Case B2) changed the predicted ACES and AHEP magnitudes from those computed where the HVAC system capacity was allowed to be sized internally by DOE 2.1B. While the magnitude shifts between Cases B1 and B2, as shown in Figure 4.8, are not extreme, the results indicate that predicted energy savings and penalty (ACES + AHEP) are dependent on HVAC system specification.

The third case, designated as B3, involved a change in HVAC operating schedule. The HVAC system capacity was again forced to

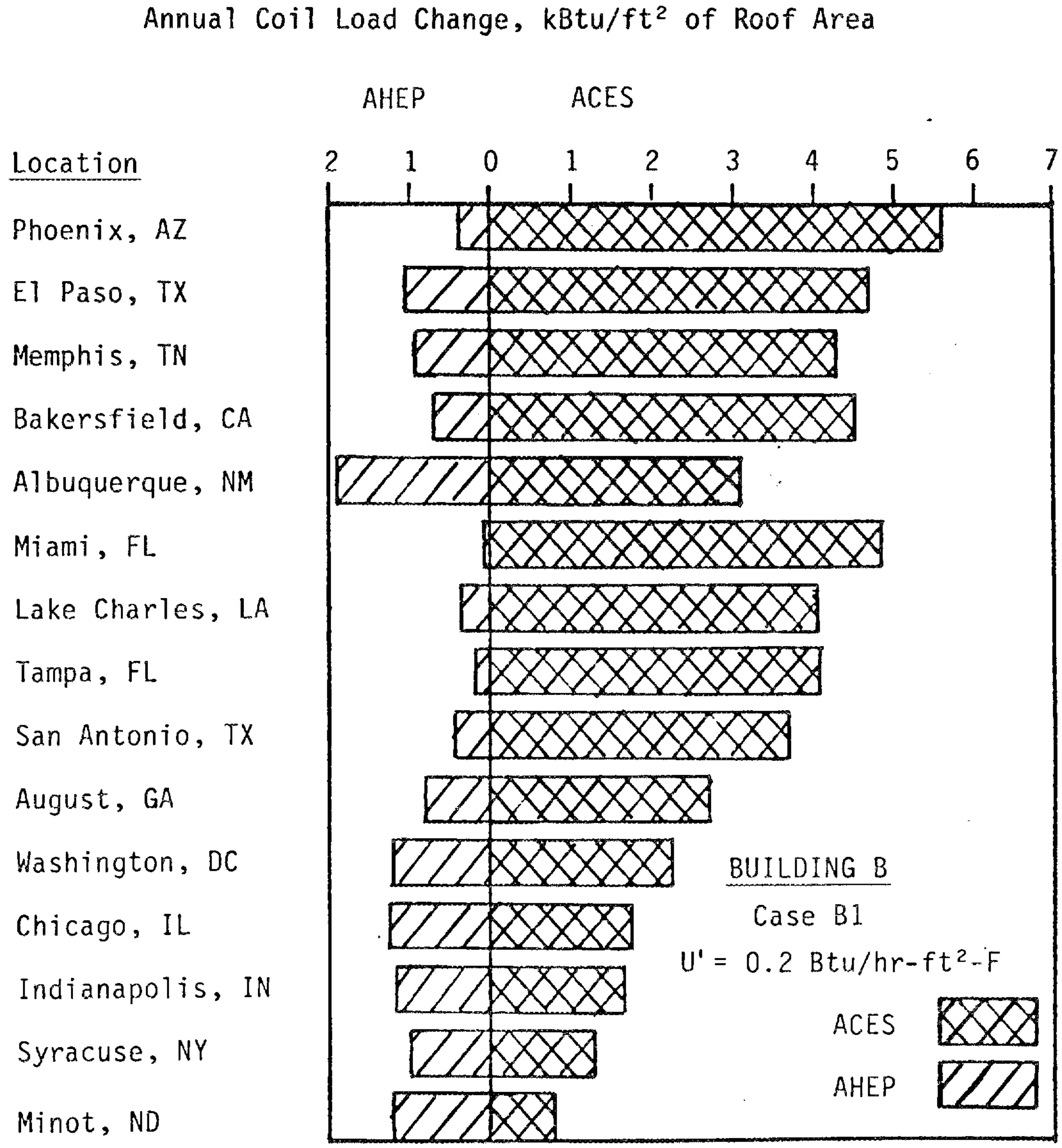

Figure 4.5 Comparison of HVAC Coil Load Changes (AHEP and ACES) Predicted by DOE 2.1B Systems for Building B (Case B1) Due to a Lowering of Roof's Solar Absorptance from 0.8 to 0.3

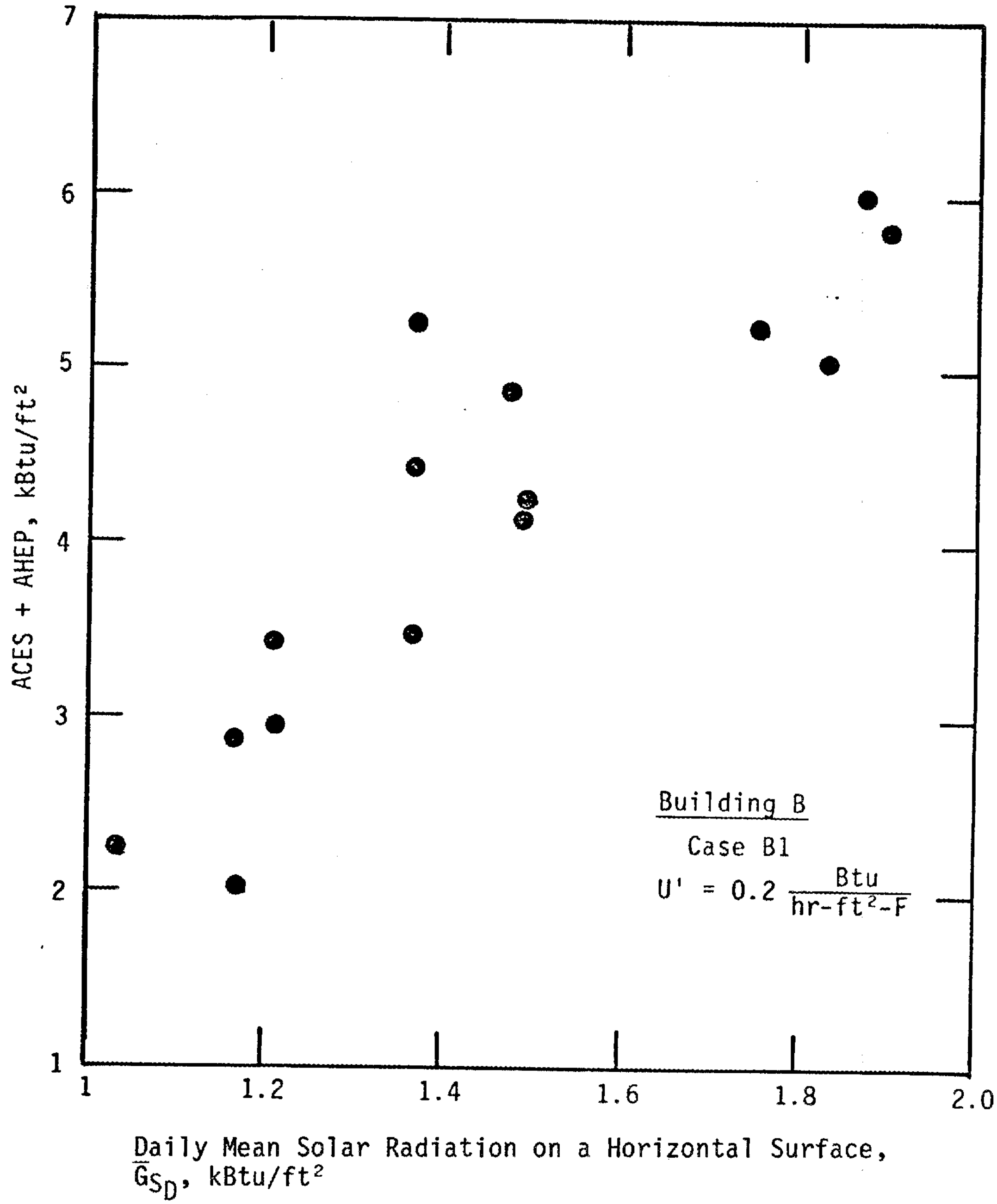

Figure 4.6 Illustration of Variation of (ACES + AHEP) with the Daily Mean Solar Radiation on a Horizontal Surface (Case B1 for Building B with $U' = 0.2$ Btu/hr-ft^2-F)

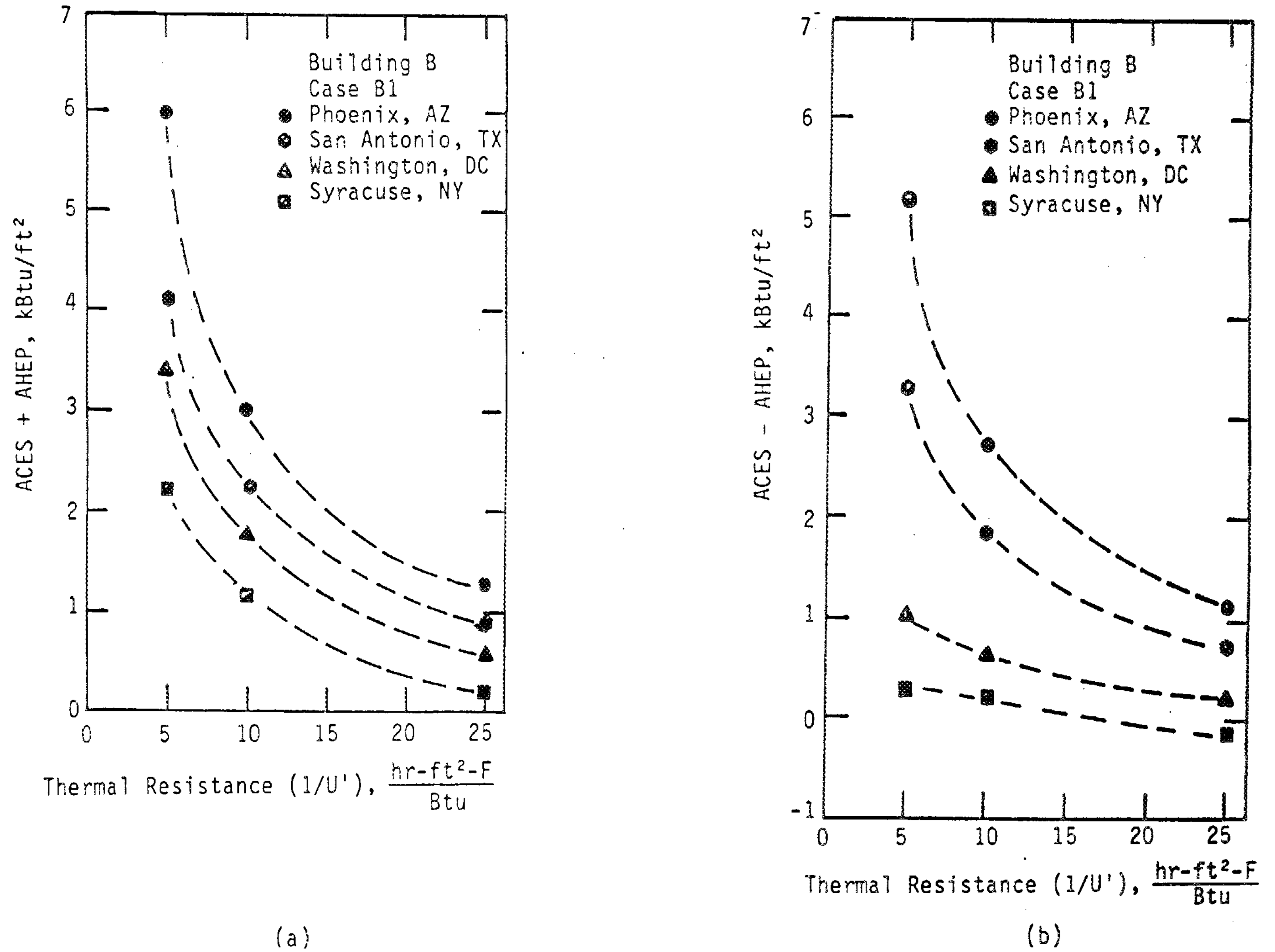

Figure 4.7 Illustration of the Effect of Thermal Resistance on Computed (ACES + AHEP) and the Difference (ACES - AHEP) for Case B1 of Building B

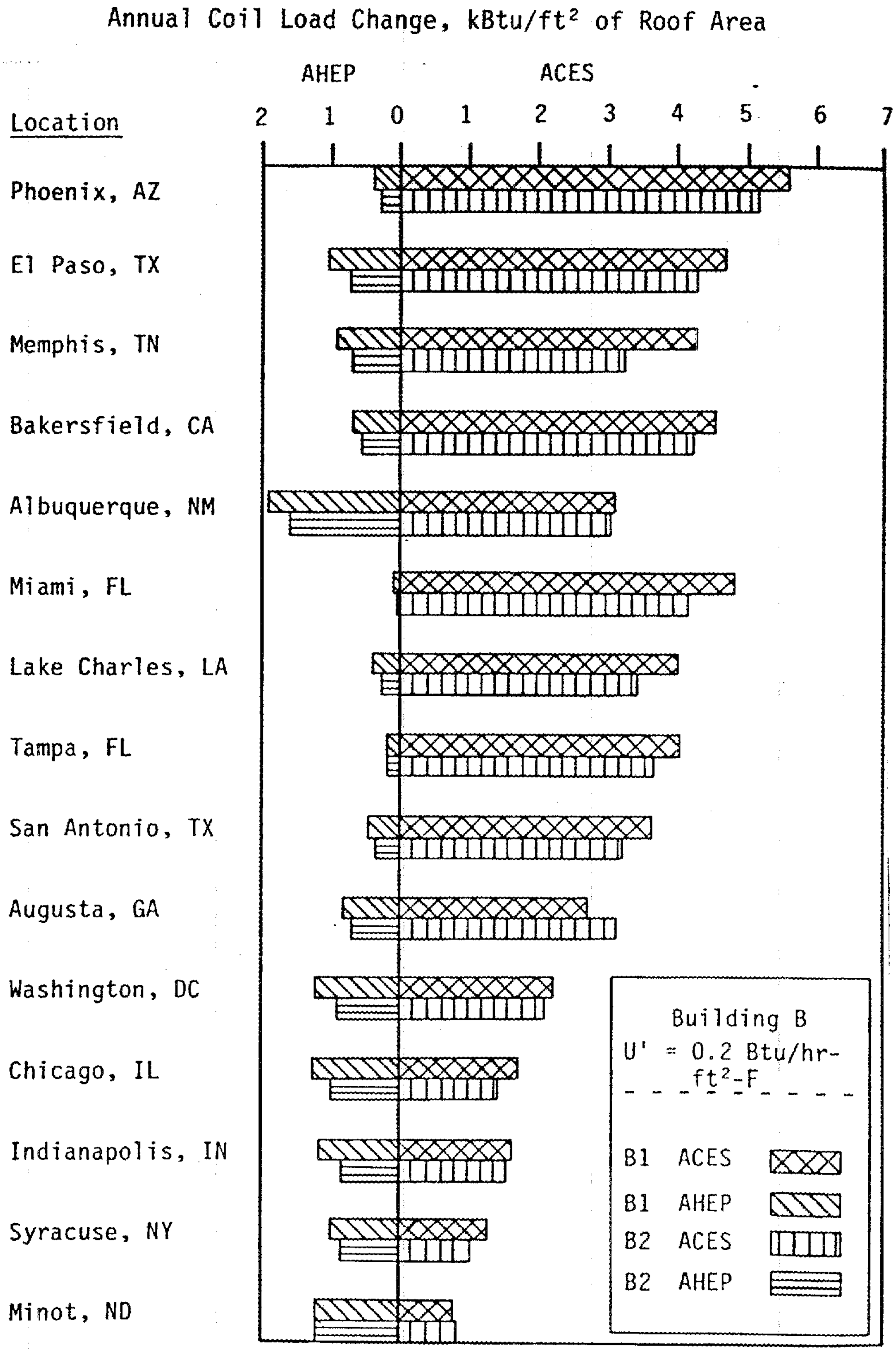

Figure 4.8 HVAC Coil Load Changes (ACES and AHEP) Predicted by DOE 2.1B for Cases B1 and B2 of Building B Resulting from Lowering the Roof's Solar Absorptance from 0.8 to 0.3

be the same for the $\alpha = 0.3$ case as that generated by DOE 2.1B for the $\alpha = 0.8$ case. Internal loads (people, lights, and equipment) were scheduled only during the day for weekdays, but the HVAC system was scheduled to operate continuously. Nighttime and weekend setback was not employed. For twenty locations, predicted changes in cooling coil load, heating coil load, electrical energy required by the system fan and the electrical energy required by the cooling system are tabulated in Appendix F, Table F.8. The change in fan requirements are zero because the fan was scheduled to operate continuously in Case B3. The predicted coil load increments (ACES and AHEP) are depicted in Figure 4.9 where the results for Case B2 are repeated for comparison. Comparing results for Cases B2 and B3 shows the effect of changing the HVAC operating schedule. The results show that maintaining the space conditioned continuously causes an increase in both predicted ACES and AHEP values. The increase can probably be explained by the fact that weekend operation is included and that the space was conditioned at night where some time-delayed energy transfer may also be included during a regular work day.

The effect of solar loading on a roof's surface temperature is influenced by the exterior heat transfer coefficient. All of the previously discussed computations were made using the DOE 2.1B incorporated correlation of h_o with wind speed that corresponds to a rough surface (refer to Appendix C). An additional set of calculations were made for Building B with conditions being the same as those used for Case B3 except for the h_o correlation. The code was changed to make use of the h_o correlation designated for a very smooth surface. This set of computer runs is designated as Case B4. For twenty locations, predicted changes in cooling coil load, heating coil load, electrical energy required by the system fan and the electrical energy required by the cooling system are tabulated in Appendix F, Table F.9. The coil load changes, ACES and AHEP, are shown in Figure 4.10 where the results for Case B3 are repeated for comparison. The comparison shows that using lower h_o values markedly increased both ACES and AHEP. This contrast indicates the important role that the surface heat transfer coefficient plays in the surface energy balance. This also indicates that the effect of solar loading on a roof can be significantly affected by wind speed since wind speed is known to effect h_o.

4.5.3 <u>Building C</u>

Calculations for the multizone office building, Building C, were made for five locations. Continuous space conditioning, involving the same scheduling as that used for Case B3, and system capacity matching were used. Predicted ACES and AHEP values for Building C are shown in Figure 4.11 together with those for Building A and Cases B1 and B2, and B3 for Building B. All cases shown in Figure 4.11 are for the common U' value of 0.2 Btu/hr-ft^2-F and the same h_o correlation, that being the one for a rough surface. ACES and AHEP values of Figure 4.11 are listed in Table 4.2 together with estimates based on the report of Chang and Busching [2]. There are two observations which comparisons of data in Figure 4.11 and Table

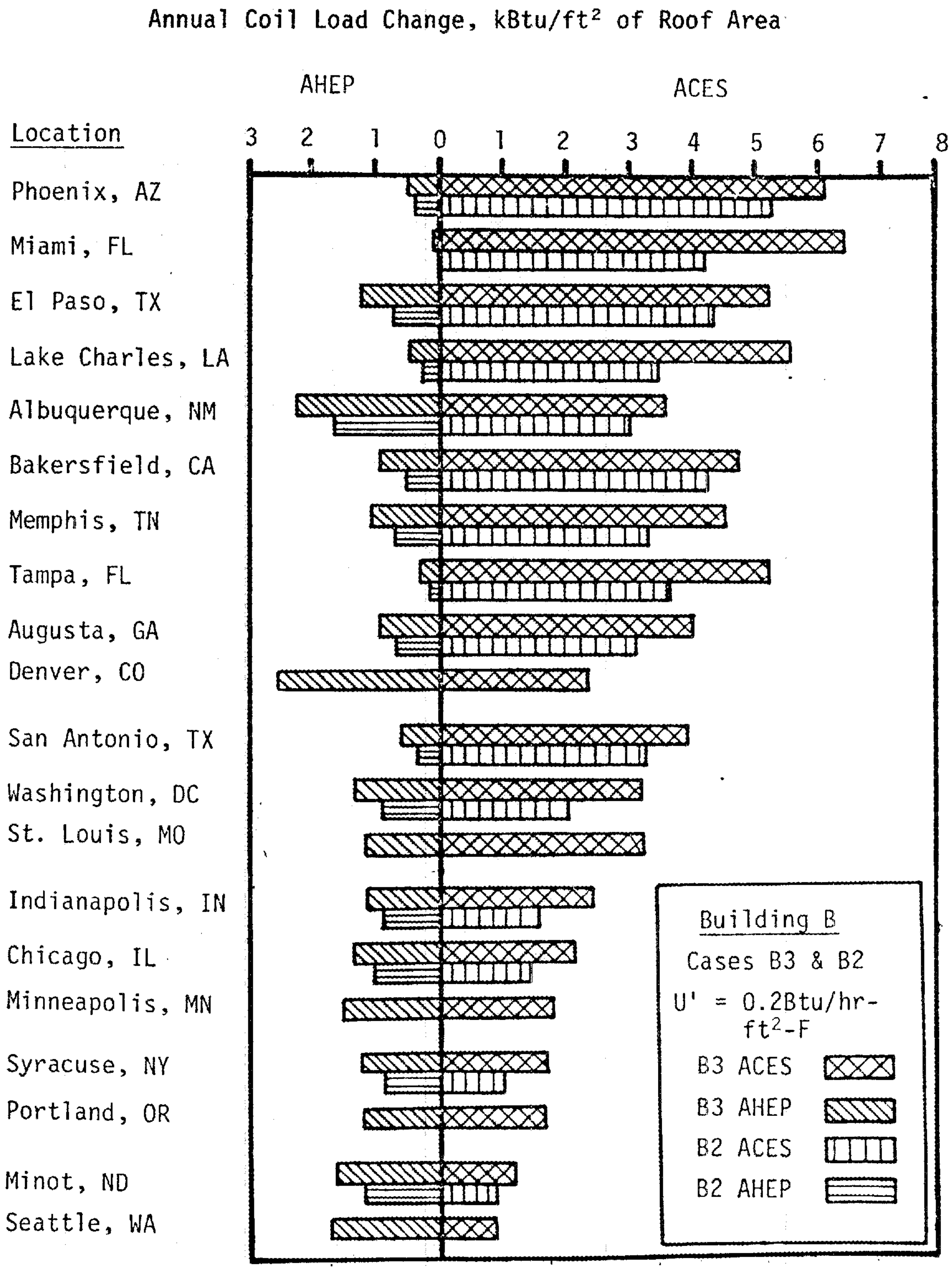

Figure 4.9 HVAC Coil Load Changes (AHEP and ACES) Predicted by DOE 2.1B Systems for Cases B3 and B2 of Building B Resulting from Lowering the Roof's Solar Absorptance from 0.8 to 0.3

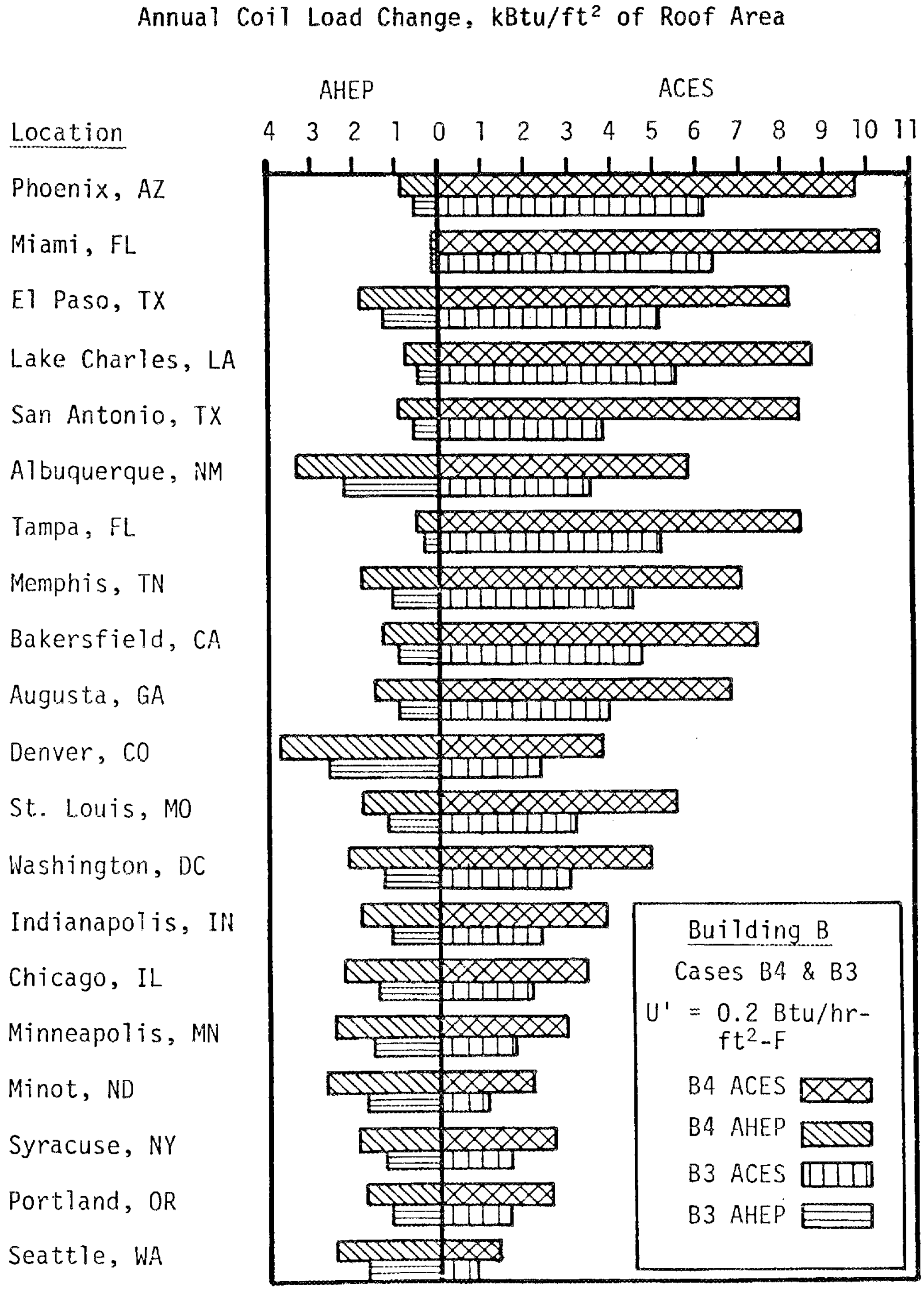

Figure 4.10 HVAC Coil Load Changes (AHEP and ACES) Predicted by DOE 2.1B Systems for Cases B4 and B3 of Building B Resulting from Lowering the Roof's Solar Absorptance from 0.8 to 0.3

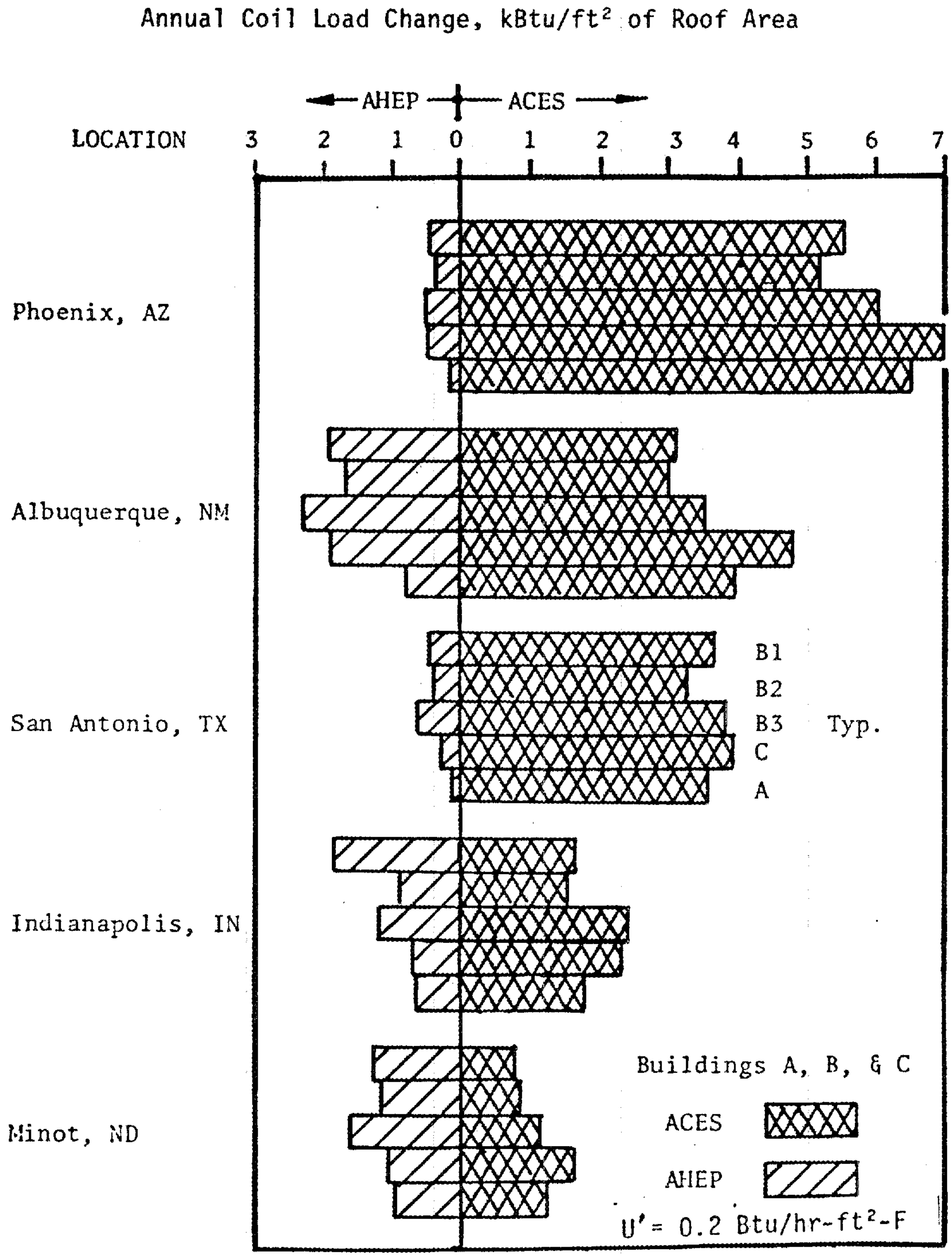

Figure 4.11 Comparisons of Annual Cooling Energy Savings (ACES) and Annual Heating Energy Penalty (AHEP) for Buildings A, B, and C. Results Based on SYSTEMS Output

Table 4.2 Annual Cooling Energy Savings (ACES) and Annual Heating Energy Penalties Predicted for a Roof Having a U' Value of 0.2 Btu/hr-ft^2-F when Its Solar Absorptance is Reduced from 0.8 to 0.3 (ACES and AHEP in kBtu/ft^2 of Roof Area)

Location	Energy Change	Chang and Busching [2]	Building and Case	A ---	B B1	B B2	B B3	C ---
Phoenix, AZ	AHEP	1312		117	417	331	497	484
	ACES	10681		6520	5581	5181	6078	7000
Albuquerque, NM	AHEP	1918		783	1903	1645	2271	1834
	ACES	8245		3977	3116	2992	3544	4834
San Antonio, TX	AHEP	931		157	426	348	594	283
	ACES	9885		3581	3692	3260	3869	3956
Indianapolis, IN	AHEP	2745		607	1176	864	1152	656
	ACES	5437		1778	1681	1557	2401	2315
Minot, ND	AHEP	3636		916	1212	1217	1617	1001
	ACES	5112		1232	800	852	1170	1676

4.2 facilitate. First, the ACES and AHEP values computed by DOE 2.1B for the buildings examined in this study are generally lower than values estimated by the data given by Chang and Busching. Second, computed magnitudes of ACES and AHEP for a particular location and for buildings having identical roofs are dependent upon building type and upon HVAC system operation. Generally, predictions follow expected trends and reveal that reduction of a roof's absorptance can be an energy conservation measure for localities of high cooling loads and high solar energy availability.

4.6 COMPARISONS OF BUILDING PREDICTIONS TO STEADY-STATE ESTIMATES

An interesting comparison can be made between steady-state estimates of(ACES + AHEP) by Equation (3.11) and DOE 2.1B predictions of (ACES + AHEP) for the building simulations considered here. The correlation of h_o versus wind speed for a rough surface listed in Appendix C was used with the mean wind speeds listed in Table 4.1 to determine h_o for the twenty locations. This $\bar{h}_o$ was used with a U' value of 0.2 Btu/hr-ft²-F to calculate U_o. Values for $\bar{G}_{S_D}$ given in Table 4.1 were used. The results of calculating the steady-state estimate of (ACES + AHEP) by Equation (3.11) are tabulated in Table 4.3. Results from DOE 2.1B for Building A and Cases B1, B2 and B3 for Building B are listed also. The percentage difference, based on the steady-state estimate, is also given. For the range of cases considered, all steady-state estimates were significantly higher than the corresponding results obtained with DOE 2.1B.

4.7 ECONOMIC CONSIDERATIONS

For investment considerations, ACES and AHEP values must be considered with respect to their ultimate impact on purchased energy. The ACES and AHEP values computed in this study represent changes in annual cooling and heating coil requirements. Utilization efficiency from source to coil must be used to determine the resultant change in energy demand at the source. The change in cooling energy at the source is given by ACES/β where β denotes the effective annual coefficient of performance for the cooling system. Likewise, the change in heating energy at the source is given AHEP/η where η denotes the effective annual heating system efficiency. For example, if β = 2.5 and η = 0.7, ACES/AHEP would have to exceed 3.57 for a resultant savings in energy at the source. The distinction in energy cost for heating and cooling must be used to determine the economic impact. For economic considerations, savings associated with an investment that occur over an extended time and which involve the time-value of money can be cast into present worth, indicates what the predicted savings represent in today's money. The present worth of an investment represents the maximum expenditure today which can be made without the investment representing a loss. The present worth of a particular ACES and AHEP combination is given by

Table 4.3 Comparison of (ACES + AHEP) for Certain Building Runs by DOE 2.1B and the Steady-State Estimate of (ACES + AHEP) by Equation (3.11) (ACES and AHEP in kBtu/ft^2 of Roof Area)

Location	(ACES+AHEP) Equation (3.11)	Building A (ACES+ AHEP)	Building A % Diff.	Building B Case B1 (ACES+ AHEP)	Case B1 % Diff.	Building B Case B2 (ACES+ AHEP)	Case B2 % Diff.	Building B Case B3 (ACES+ AHEP)	Case B3 % Diff.
Phoenix, AZ	14796	6637	55.1	5998	59.5	5512	62.8	6575	55.6
Bakersfield, CA	11718	5668	51.6	5231	55.4	4763	59.4	5656	51.7
El Paso, TX	11544	5361	53.6	5800	49.8	5017	56.5	6429	44.3
Albuquerque, NM	10090	4760	52.8	5019	50.3	4637	54.0	5815	42.4
Miami, FL	8132	3918	51.8	4885	39.9	4165	48.8	6474	20.4
San Antonio, TX	8276	3738	54.8	4118	50.2	3608	56.4	4463	46.1
Tampa, FL	8929	3858	56.8	4268	52.2	3767	57.8	5496	38.4
Augusta, GA	9280	3503	62.3	3492	62.4	3775	59.3	4936	46.8
Lake Charles, LA	7924	3396	57.1	4426	44.2	3680	53.6	5991	24.4
Memphis, TN	7816	3472	55.6	5253	32.8	3961	49.3	5603	28.3
Denver, CO	7686	3604	53.1	--	--	--	--	4838	37.1
St. Louis, MO	7223	3186	55.9	--	--	--	--	4376	39.4
Washington, DC	7518	2958	60.7	3415	54.6	2996	60.2	4426	41.1
Chicago, IL	6147	2579	58.0	2941	52.2	2430	60.5	3500	43.1
Indianapolis, IN	6667	2385	64.2	2857	57.1	2421	63.7	3553	46.7
Minneapolis, MN	6158	2312	62.4	--	--	--	--	3296	46.5
Minot, ND	6118	2148	64.9	2012	67.1	2069	66.2	5787	54.4
Syracuse, NY	5444	2015	63.0	2226	59.1	1877	62.5	2913	46.5
Portland, OR	6384	1995	68.8	--	--	--	--	2842	55.5
Seattle, WA	6113	1573	74.3	--	--	--	--	2537	58.5

$$PW = \frac{(ACES)(CEC)(PW)c}{\beta} - \frac{(AHEP)(HEC)(PWF)h}{\eta} \qquad (4.3)$$

where CEC and HEC represent current cooling energy cost and current heating energy cost, respectively. Also, $(PWF)_c$ and $(PWF)_h$ represent present-worth factors for cooling and heating, respectively. These present-worth factors depend on the life of the energy-saving modification (reduction of α here), the applicable discount rate and the escalation rate for the respective energy cost.

Determination of the present worth of an investment by Equation 4.3 requires good insight or good speculation as to the life of the investment, the discount rate and fuel escalation rates. Estimations can be made with the aid of published estimates for some of these. For example, uniform present-worth factors for ten DOE regions and averages for the United States are tabulated in Reference 16, a DOE life-cycle cost manual. Also included are mid-1983 energy costs.

Without taking the full step of estimating present worth factors, an interesting comparison of estimated savings can be made by casting the computed results into current cost savings. For this comparison, natural gas was considered to be the heating fuel, and the cooling systems were considered to be electrically driven. Use was made of mid-1983 national average costs of electrical energy and natural gas as listed in Reference 16 for the commercial sector. Electrical savings were taken as the computed savings in electrical cooling energy plus the savings in HVAC fan energy. In doing this, the DOE 2.1 generated HVAC system coefficient of performance was automatically taken into account. DOE 2.1B incorporates a system performance curve which is affected by local climatic variables. An electrical energy cost of 6.226 ¢/Kw-hr was used. Heating by natural gas was assumed with an efficiency of 70 percent and a fuel cost of 5.58 $\$/10^6$ Btu. Results of this cost evaluation are tabulated in Table 4.4. Largest savings occur for locations with large average daily solar radiation and characterized by large cooling requirements. All cases presented for comparison in Table 4.4 correspond to a roof U'-value of 0.2 Btu/hr-ft^2-F. Use of larger U' values will result in smaller savings and vice versa. For the range of cases compared here, it is noted that the upper bound on calculated current annual savings per square foot of roof area is of the order of the cost of 1 kw-hr of electrical energy. This magnitude is based on a heating system efficiency of 70 percent, and a ratio of electrical energy cost to heating energy cost of 3.27:1.

5. SUMMARY WITH CONCLUSIONS AND RECOMMENDATIONS

5.1 SUMMARY

The computer code, DOE 2.1B, was used to calculate changes in a building's cooling and heating energy requirements occurring with a reduction in the roof's solar absorptance from 0.8 to 0.3. With

Table 4.4 Comparative Annual Cost Savings Resulting from Lowering a Roof's Absorptance from 0.8 to 0.3. Values Are Given in cents/ft^2 and Are Based on Electrical Energy Cost of 6.226¢/Kw-hr and Heating with Natural Gas Costing 5.58$/10^6 Btu at an Efficiency of 70%*. All Cases Are for a Roof Having a U' Value of 0.2 Btu/hr-ft^2-F.

Location	Bldg. A ---	Bldg. B Case B1	Bldg. B Case B2	Bldg. B Case B3	Bldg. B Case B4	Bldg. C ---
Phoenix, AZ	5.72	6.75	3.79	3.37	5.37	3.96
Bakersfield, CA	4.75	5.16	3.01	2.34	3.75	--
El Paso, TX	4.43	5.56	2.80	2.06	3.32	--
Albuquerque, NM	3.17	1.75	0.64	0.43	0.87	1.59
Miami, FL	3.25	4.16	2.66	3.54	5.48	--
San Antonio, TX	2.86	3.51	2.13	1.99	3.98	2.29
Tampa, FL	3.12	3.50	2.28	2.62	3.95	--
Augusta, GA	3.03	2.28	1.65	1.63	2.99	--
Lake Charles, LA	1.80	3.92	2.11	2.70	4.21	--
Memphis, TN	2.28	3.32	1.63	1.66	2.59	--
Denver, CO	1.80	--	--	-0.51	-0.55	--
St. Louis, MO	1.89	--	--	0.85	1.63	--
Washington, DC	1.25	1.52	0.51	0.74	1.10	--
Chicago, IL	0.71	0.62	0.01	0.2	0.36	--
Indianapolis, IN	0.90	1.17	0.24	0.60	0.93	0.94
Minneapolis, MN	0.38	--	--	-0.11	-0.09	--
Minot, ND	0.39	-0.55	-0.53	-0.52	-0.76	0.31
Syracuse, NY	0.42	0.21	-0.14	0.08	0.13	--
Portland, OR	0.72	--	--	0.76	0.29	--
Seattle, WA	0.34	--	--	-0.79	-1.04	--

*Cost Values were taken from Reference 16. They represent mid-1983 national averages for the commercial sector.

the same flat roof construction for comparable thermal resistances, three different buildings were examined. In two cases, three levels of roof thermal resistance were considered. Computations were made for up to twenty different locations within the United States. Reported changes in energy use are based on the output of the SYSTEMS subprogram of DOE 2.1B. Predicted cooling-energy savings and heating-energy penalties are included in tabular form and are comparatively presented for representative cases by bar charts. For the lowest level of roof thermal resistance considered, the results have been cast into estimated annual cost savings using one combination of cooling and heating energy costs.

A brief literature review is also outlined noting the work of others where attention has been given to claimed advantages of using roofs with low solar absorptance; the advantages are reported to be reduced surface temperature swings and savings in the energy required for cooling. This work focused on the energy savings.

5.2 OBSERVATIONS AND LIMITATIONS

Exact magnitudes of changes in heating and cooling energy which occur when a roof's solar absorptance is lowered are affected by building construction, HVAC system scheduling and operation, thermal resistance of the roof and local climatic conditions. The majority of ACES and AHEP comparisons depicted in this work correspond to a roof U' value of 0.2 Btu/hr-ft^2-F. Sufficient calculations were made, however, to show that energy savings are reduced as the thermal resistance of the roof increases. The savings follow the general trend of varying inversely with thermal resistance.

The sunlit-surface energy balance algorithm incorporated within DOE 2.1B accommodates user modification of the surface's solar absorptance, but the option for simultaneously altering the infrared emittance is not available. When a roof's solar absorptance is lowered, it is likely that its infrared emittance will also be lowered. A reduced infrared emittance will affect long wavelength radiative transfer to the sky. This effect has not been quantified in this study.

Calculations were made for a specific reduction of α from 0.8 to 0.3. This seems to represent an upper limit on the change, particularly from a practical viewpoint. However, no information is available on the effective life of reflective materials and coatings. Dirt and other environmental influences can cause a reduction in the reflective properties. Also, the influence of such factors as water ponding, snow, and roof-mounted equipment has not been considered.

The calculated results were shown to be strongly dependent on the value used for the surface convective heat transfer coefficient. The rather simplistic models that are used in the computational algorithms need to be evaluated for real building situations. For a roof that is well insulated, the external film heat transfer coefficient does not affect the total energy transfer significantly. For surface temperature prediction and for accurate determination of the change in heat transfer affected by the energy balance at the surface, the need for an accurate external heat transfer coefficient is much more essential.

5.3 CONCLUSIONS

Conclusions offered here are based on the limitations of this study as outlined above.

(1) Annual energy savings can be realized, particularly for locations characterized by large mean daily global solar radiation and large building cooling requirements.
(2) Annual energy savings for a real building are less than steadystate estimates.
(3) For a flat roof having a thermal resistance of about 5 ft^2-hr-F/Btu, the order of magnitude of the maximum possible annual savings is equivalent to the cost of one kw-hr of electrical energy per square foot of exposed roof area when heating is done with gas and cooling is done with an electrically driven system.
(4) Annual energy savings vary inversely with the magnitude of the roof's thermal resistance.
(5) Annual energy savings may be almost twice as large for a roof where the exterior heat transfer coefficient is governed by smooth-surface correlations as for one governed by the rough-surface correlation.
(6) Exact magnitudes of savings for the same building vary with HVAC sizing and operational schedule.

5.4 RECOMMENDATIONS

This study has shown that use of reflective roofs can result in energy savings, but the exact magnitudes of the savings appear to depend sufficiently on operating conditions such that more work is needed to quantify the relative contribution of the different influences. Consideration of how changing a roof's absorptance affects the infrared emittance and how this in turn affects the energy use needs more study. Attention should be given to the useful life of reflective coatings. The effect of reduced surface temperature swings on membrane life is worthy of further study. With these concerns in mind, the following specific recommendations are given.

(1) Examine the effect of a reduced infrared emittance simultaneously with a reduced solar absorptance on calculated ACES and AHEP values.
(2) Study how the radiative properties of a roof's surface change with environmental exposure.
(3) Investigate in more detail how the convective heat transfer coefficient on roofs varies with environmental parameters.

(4) Study the effects on the performance of roof coverings caused by reduction in surface temperature swing that occur when reflective roofs are used.

6. REFERENCES

1. J. N. Robinson, "The Assessment of Roofing Research--An Interim Report," ORNL/TM-7460, Oak Ridge National Laboratory, July 1981.

2. T. Chang, and H. W. Busching, "Energy Savings Potential of Roofing Research," ORNL/Sub/82-22293/1, report prepared under Purchase Order No. 19X22293V for ORNL by Clemson University, December 1983.

3. S. D. Probert, and T. J. Thirst, "Design and Performance of Roofs," Applied Energy, 6, 1980, pp. 79-97.

4. M. C. Baker, ROOF--Design, Application, and Maintenance, sponsored by the National Research Council of Canada, Multiscience Publications Limited, 1980.

5. J. A. Reagan, and D. M. Acklam, "Solar Reflectivity of Common Building Materials and Its Influence on the Roof Heat Gain of Typical Southwestern USA Residences," Energy and Buildings, 2, 1979, pp. 237-248.

6. S. G. Talbert, "Energy Savings of Buildings Using Aluminum Roof Flakes," Energy Savings Report, prepared by Battelle Columbus Laboratories, Columbus, Ohio, for Transmet Corporation, Columbus, Ohio.

7. DOE-2 Reference Manual--Parts 1 and 2, prepared for the U. S. Department of Energy under Contract W-7405-ENG-8, Lawrence Berkely Laboratory and Los Alamos National Laboratory LA-7689-M Ver. 2.1, LBL-8706, Rev. 1, May 1980.

8. W. J. Rossiter, Jr., and R. G. Mathey, "Effect of Insulation on the Surface Temperature of Roof Membranes," National Bureau of Standards, NBSIR 76-987, February 1976.

9. E. C. Shuman, "Field Measurements of Heat Flow through a Roof with Saturated Thermal Insulation and Covered with Black and White Granules," Thermal Insulation Performance, ASTM STP 718, D. L. McElroy and R. P. Tye, Eds., American Society for Testing and Materials, 1980, pp. 519-539.

10. J. R. Keeton, and R. L. Alumbaugh, "Energy Factors and Temperature Distribution in Insulated Built-Up Roofs," TN N-1600,

Civil Engineering Laboratory, Naval Construction Battalion Center, Port Hvenenee, California, February 1981.

11. ASHRAE Handbook--1981 Fundamentals, American Society of Heating, Refrigerating and Air-Conditioning Engineers, Inc., Atlanta, Georgia, 1981.

12. F. S. Dubin, and C. G. Long, Jr., Energy Conservation Standards for Building Design Construction and Operation, McGraw-Hill Book Company, 1978.

13. C. W. Griffin, "Cost Savings with Heat-Reflective Roof Coatings," Plant Engineering, July 10, 1980, pp. 98-102.

14. C. L. Knapp, T. L. Stoffel, and S. D. Whitaker, "Insulation Data Manual," SERI/SP-755-789, October 1980.

15. "Wind Energy Resource Atlas," PNL-3195-WERA 1 through 9, Volumes 1 through 9, 1980-1983.

16. Federal Energy Management Program Life Cycle Cost Manual (NBS 135) Update, DOE/CE-0076, March 1984, U. S. Department of Energy, Washington, D.C.

APPENDIX A

PUBLISHED ABSORPTANCE VALUES FOR VARIOUS BUILDING MATERIALS AND SURFACE COATINGS

APPENDIX A

PUBLISHED ABSORPTANCE VALUES FOR VARIOUS BUILDING MATERIALS AND SURFACE COATINGS

Included in Tables A.1 through A.10 of this appendix are values of reflectance and absorptance for building materials found in the literature. Table A.9 also lists reported thermal emittance values.

Table A.1 Solar Absorptance Values Given in Table 2 of Reference 3

	Surface color	Absorptance
	Black	0.95
	Dark grey	0.85
	Light grey	0.65
	White	0.45
	Copper-tarnished	0.80
Weathered Metals	Copper-oxidized	0.65
	Aluminum	0.60
	Galvanized iron	0.90

Table A.2 Solar Absorptance Values Recommended in Reference 4 (Table 5.5 in Reference 4)

Item	Absorptance
Surface Color	
Black	0.95
Dark grey	0.80
Light Grey	0.65
White	0.45
Weathered Roofing	
Copper	0.65
Aluminum	0.60
Galvanized Iron	0.90
Asbestos-Cement	0.80
Smooth-surface Asphalt	0.93
Grey Gravel	0.75
White Gravel	0.50
Concrete Paving	0.65

Table A.3 Solar Reflectance and Absorptance for Walls Made of Concrete and Adobe Blocks (From Table 1 of Reference 5)

Description	Reflectance	Absorptance
Burnt adobe block, running bond,		
tooled light grey mortar joint	0.36	0.64
Same with raked joint	0.34	0.66
Colored slump block, running bond,		
concave low contrast mortar joint		
Tan (San Xavier SX-15)	0.43	0.57
Plain (San Xavier SX-16)	0.44	0.56
Buff (Columbia Block)	0.39	0.61
Santa Rosa (Columbia Block)	0.36	0.64
Palo Verde (San Xavier SX-17)	0.33	0.67
Coral (San Xavier SX-14)	0.38	0.62
Adobe Red (Columbia Block)		
with raked joint	0.21	0.79
Colored CMU (concrete masonry unit)		
running bond, concave low contrast		
mortar joint		
Coral (San Xavier SX-14)	0.34	0.66
Adobe Red (San Xavier SX-26)	0.32	0.68
Buff (Columbia Block)	0.31	0.69
Plain or grey	0.39	0.61
Same with plain joint	0.45	0.55

Table A.4 Solar Reflectance and Absorptance for Walls Made of Bricks (From Table 2 of Reference 5)

Description	Reflectance	Absorptance
Brown (PBY* color #19) scratch brick common bond, concave medium grey mortar joint	0.28	0.72
Same color ruffled brick, basket weave bond, same color and type joint	0.36	0.64
Same with herringbone bond	0.33	0.67
Light red (PBY color #16) scratch brick, common bond, concave medium grey mortar joint	0.38	0.62
Orange (PBY color #06) ruffled brick, plain medium grey mortar joint	0.41	0.59
Buff (PBY color #94) plain brick, stack bond stretchers, raked medium grey mortar joint	0.51	0.49
Same color ruffled brick, English cross bond, concave medium grey mortar joint	0.43	0.57
Same color scratch brick, running bond, plain medium grey mortar joint	0.41	0.59
Red (PBY color #04) ruffled brick, third bond oversize brick, raked medium grey mortar joint	0.35	0.65
Same color and type brick, English cross bond, concave medium grey mortar joint	0.34	0.66

Table A.5 Solar Reflectance and Absorptance of Painted and Coated Walls (From Table 3 of Reference 5)

Description	Reflectance	Absorptance
Painted slump block, running bond, concave joint		
Pearl White (Pioneer Paints)	0.74	0.26
Navaho White (Pioneer Paints)	0.70	0.30
White (Pioneer Paints)	0.71	0.29
Spanish White (Pioneer Paints)	0.68	0.32
Egg Shell White (Pioneer Paints)	0.65	0.35
Mortar washed, solid grey coverage on slump block, same bond and joint	0.49	0.51
Painted CMU (concrete masonry unit), same bond and joint		
Bone White (Southwestern Paints)		
Navaho White (Pioneer Paints)	0.72	0.28
Sea Shell Beige (Pioneer Paints)	0.55	0.45
Pearl White (Pioneer Paints)	0.69	0.31
Desert Sand (Sears Roebuck & Co.)	0.42	0.58
Painted stucco,		
Bone White (Southwestern Paints)	0.65	0.35
Painted wood paneling		
Avocado Green (Pioneer Paints)	0.15	0.85
Sand Dune (Pioneer Paints)	0.26	0.74
Beige (brand unknown)	0.40	0.60
Stained wood paneling		
Weathered Brown (2310 Southwestern's wood stain)	0.10	0.90
Dark Brown (2302 Southwestern's wood stain)	0.13	0.87

Table A.6 Solar Reflectance and Absorptance of Shingled Roofs (From Table 4 of Reference 5)

Description	Reflectance Value (%)
Asphalt tab shingles, common lay	
Woodblend (GAF)	17
Russet Blend (GAF)	9
Autumn (Flintkote)	10
Frosted Red (Flintkote)	20
Canyon Red (Flintkote)	13
Snow White (Flintkote)	24
Dark Mahogany (GAF)	8
Pastel Green (GAF)	16
Earthtone Brown (GAF)	9
Blizzard (Fire King)	34
White (JM)	33
Red (JM)	14
Clover Green (Flintkote)	11
Shake cedar wood shingles, new, unoiled	32
Same but oiled	28
Red clay mission tile	26

Table A.7 Solar Reflectance and Absorptance of Coated and Built-up Roofs (From Table 5 of Reference 5)

Description	Reflectance	Absorptance
Pea gravel covered		
Dark blend	0.12	0.88
Medium blend	0.24	0.76
Light blend	0.34	0.66
White coated	0.65	0.35
Crushed used brick, red, covered	0.34	0.66
White marble chips covered	0.49	0.51
Flexstone or mineral chip roof type, white	0.26	0.74
Polyurethane foam, white coated	0.70	0.30
Same with tan coating	0.41	0.54
Silver, aluminum painted tar paper	0.51	0.49
White coated, smooth, Kool Kote (Corbett Roofing Co./Tucson)	0.75	0.25
Tarpaper, "weathered"	0.41	0.59

Table A.8 Color Classification for Opaque Building Materials (From Table 7 of Reference 5)

Color code	Solar Reflectance	Solar Absorptance
Very light	0.75	0.25
Light	0.65	0.35
Medium	0.45	0.55
Dark	0.25	0.75
Very dark	0.10	0.90

Very light:	Smooth building material surfaces covered with a fresh or clean stark white paint or coating
Light:	Masonry, textured, rough wood, or gravel (roof) surfaces covered with a white paint or coating
Medium:	Off-white, cream, buff or other light colored brick, concrete block, or painted surfaces and white-chip marble covered roofs
Dark:	Brown, red or other dark colored brick, concrete block, painted or natural wood walls and roofs with gravel, red tile, stone, or tan-to-brown shingles
Very dark:	Dark brown, dark green or other very dark colored painted, coated, or shingled surfaces

Table A.9 Values of Solar Reflectance, Solar Absorptance and Thermal Emittance for Several Samples of Materials Used on Roofs (From Table 1 of Reference 6)

Sample Number	Sample Description	Solar Reflectance	Solar Absorptance	Thermal Emittance
1	Trocal SMA (PVC base)	0.285	0.715	0.84
2	Derbigum HPS (Modified Bitumen)	0.58	0.942	0.83
3	Aluminum Membrane (KMM)	0.715	0.285	0.31
4	Sure Seal, Design A (EPDM)	0.124	0.876	0.86
5	SPM System (EPDM)	0.108	0.892	0.87
6	Awaplan Regular (Modified Bitumen)	0.067	0.933	0.89
7	Awaplan Welding (Modified Bitumen)	0.244	0.756	0.88
8	SPM 60 (EPDM)	0.076	0.924	0.84
15	Aluminum Fiber Coating, 1.5#	0.53	0.47	0.51
16	Aluminum Fiber Coating, 3.0#	0.364	0.636	0.61
17	Rolled Aluminum Flake	0.695	0.305	0.23
18	Unrolled Aluminum Flake	0.584	0.416	0.28
19	Rolled Coated Aluminum Flake	0.542	0.458	0.32
20	Unrolled Coated Aluminum Flake	0.536	0.464	0.31
21	Plain Steep Asphalt	0.156	0.844	0.77
22	Gravel Coated Asphalt	0.234	0.766	0.74

Table A.10 Solar Absorptance Values for Various Exterior Surfaces (From Chapter III of Reference 7)

Material	Absorptance	Paint	Absorptance
Black concrete	0.91	Optical flat black paint	0.98
Stafford blue brick	0.89	Flat black paint	0.95
Red brick	0.88	Black lacquer	0.92
Bituminous felt	0.88	Dark gray paint	0.91
Blue gray slate	0.87	Dark blue lacquer	0.91
Roofing, green	0.86	Black oil paint	0.90
Brown concrete	0.85	Dark olive drab paint	0.89
Asphalt pavement, weathered	0.82	Dark brown paint	0.88
Wood, smooth	0.78	Dark blue-gray paint	0.88
Uncolored asbestos cement	0.75	Azure blue or dark green lacquer	0.88
Uncolored concrete	0.65	Medium brown paint	0.84
Asbestos cement, white	0.61	Medium light brown paint	0.80
White marble	0.58	Brown or green lacquer	0.79
Light buff brick	0.55	Medium rust paint	0.78
Built-up roof, white	0.50	Light gray oil paint	0.75
Bituminous felt, aluminized	0.40	Red oil paint	0.74
Aluminum paint	0.40	Medium dull green paint	0.59
Gravel	0.29	Medium orange paint	0.58
White on galvanized iron	0.26	Medium yellow paint	0.57
White glazed brick	0.25	Medium blue paint	0.51
Polished aluminum reflector sheet	0.12	Medium kelly green paint	0.51
Aluminized mylar film	0.10	Light green paint	0.47
Tinned surface	0.05	White semi-gloss paint	0.30
		White gloss paint	0.25
		Silver paint	0.25
		White lacquer	0.21
		Laboratory vapor deposited coatings	0.02

APPENDIX B

ACES AND AHEP VALUES BASED ON REFERENCE 2

APPENDIX B

ACES AND AHEP VALUES BASED ON REFERENCE 2

In their assessment of the energy-saving potential of roofing research, Chang and Busching [2] estimated the roof area for the zones depicted in Figure B.1. They used Dubin's [12] nomographs, which accommodated making estimates for α of 0.8 and 0.3, to calculate the total heat gains and losses for each zone for roof U values of 0.2, 0.16, 0.12, 0.08 and 0.04 Btu/hr-ft^2-F. The gains and losses reported by Chang and Busching were used to determine ACES and AHEP values for each of the zones indicated in Figure B.1. The results are tabulated for reference in Table B.1 for the U values of 0.2 and 0.04 Btu/hr-ft^2-F.

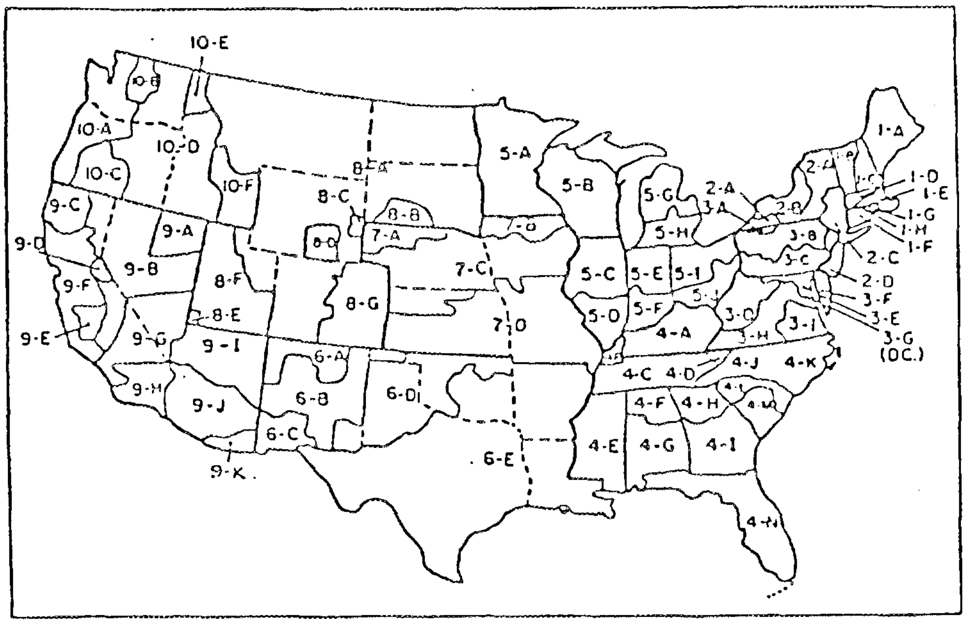

Figure B.1 Weather Zones in the Ten U.S. Federal Regions (From Reference 2)

Table B.1 Annual Cooling Energy Savings (ACES) and Annual Heating Energy Penalties (AHEP) Based on the Report by Chang and Busching [2] (All annual energy values are per ft² of roof area.)

Weather Zone Designation	U' = 0.2 Btu/hr-ft²-F ACES (Btu/ft²)	U' = 0.2 Btu/hr-ft²-F AHEP (Btu/ft²)	U' = 0.04 Btu/hr-ft²-F ACES (Btu/ft²)	U' = 0.04 Btu/hr-ft²-F AHEP (Btu/ft²)
1-A	4366	5331	255	1755
1-B	4704	5323	243	1752
1-C	4709	5328	236	1754
1-D	4898	3997	254	981
1-E	4874	499	393	733
1-F	4875	1076	396	670
1-G	4878	3343	395	667
1-H	4882	3307	394	709
2-A	4689	4818	235	1360
2-B	4689	4212	233	1106
2-C	4875	3746	393	1106
2-D	5435	2952	511	746
3-A	4722	3819	278	1319
3-B	4876	3436	395	1054
3-C	5112	2777	417	997
3-D	5436	2699	510	584
3-E	5436	2644	511	962
3-F	5435	2491	510	707
3-G	5433	2684	503	1048
3-H	5743	2181	749	1011
3-I	5994	1921	743	640
4-A	5994	2304	696	545
4-B	6871	2251	936	1082
4-C	6852	1769	928	674
4-D	6140	2105	1134	945
4-E	8039	1285	1391	616
4-F	7430	1850	1250	888
4-G	7962	1312	1391	719
4-H	7429	1742	1206	822
4-I	7964	1424	1390	719
4-J	6589	2157	881	759
4-K	6870	1687	928	887
4-L	7151	1645	1045	841
4-M	7778	1312	1136	739
4-N	8177	706	1392	602

Table B.1 (continued)

Weather Zone Designation	U' = 0.2 Btu/hr-ft²-F ACES (Btu/ft²)	U' = 0.2 Btu/hr-ft²-F AHEP (Btu/ft²)	U' = 0.04 Btu/hr-ft²-F ACES (Btu/ft²)	U' = 0.04 Btu/hr-ft²-F AHEP (Btu/ft²)
5-A	4874	4564	394	2311
5-B	4689	4162	233	1276
5-C	5436	1173	510	1084
5-D	6272	16174	764	5261
5-E	5437	2745	510	1131
5-F	5813	2925	559	775
5-G	4687	4316	235	1285
5-H	4875	3734	393	1054
5-I	5112	3358	418	1002
5-J	5437	2799	511	746
6-A	6545	1977	1159	909
6-B	8245	1918	1391	718
6-C	7091	1682	909	500
6-D	7987	1703	1276	656
6-E	9885	931	1924	400
7-A	5548	3161	645	1355
7-B	5434	3500	510	1356
7-C	6157	2855	812	978
7-D	7033	2563	907	1011
7-E	7143	2908	982	759
8-A	5112	3636	417	1387
8-B	5490	3529	588	980
8-C	5000	3000	1000	2000
8-D	4674	3913	217	1087
8-E	6077	2421	728	975
8-F	8710	1613	1613	968
8-G	5855	2747	716	851
9-A	6250	3000	750	1500
9-B	6685	1889	930	694
9-C	6027	2443	411	913
9-D	8239	2453	1447	1006
9-E	8127	1216	1419	695
9-F	6317	1607	812	412
9-G	7944	1481	1412	616
9-H	12719	395	3176	569
9-I	6620	1480	950	615
9-J	10681	1312	2267	717
9-K	8602	1326	1505	717

Table B.1 (continued)

Weather Zone Designation	U' = 0.2 Btu/hr-ft²-F ACES (Btu/ft²)	U' = 0.2 Btu/hr-ft²-F AHEP (Btu/ft²)	U' = 0.04 Btu/hr-ft²-F ACES (Btu/ft²)	U' = 0.04 Btu/hr-ft²-F AHEP (Btu/ft²)
10-A	4707	2721	162	966
10-B	4686	4136	231	1343
10-C	4865	2962	404	1288
10-D	5113	3540	417	933
10-E	5079	4074	423	1323
10-F	5106	4206	397	1270

APPENDIX C

CORRELATIONS FOR h_o USED IN DOE 2.1B

APPENDIX C

CORRELATIONS FOR h_o USED IN DOE 2.1B

Six different correlations of h_o with wind speed are incorporated in DOE 2.1B. They are coded by numerals 1 though 6 with 1 corresponding to a rough surface and 6 to a smooth surface. For reference the correlations are listed below and are shown plotted in Figure C.1.

$$h_o = A + BV + CV^2 \qquad \text{(C.1)}$$

The coefficient h_o is in Btu/hr-ft²-F when V is in mph and values of A, B and C given in Table C.1 are used.

Table C.1 Constants for Equation (C.1)

DOE 2.1B Roughness Code	A	B	C
1	2.04	0.465	0
2	2.20	0.321	0.001
3	1.90	0.330	0
4	1.45	0.315	-0.002
5	1.80	0.244	0
6	1.45	0.262	-0.001254

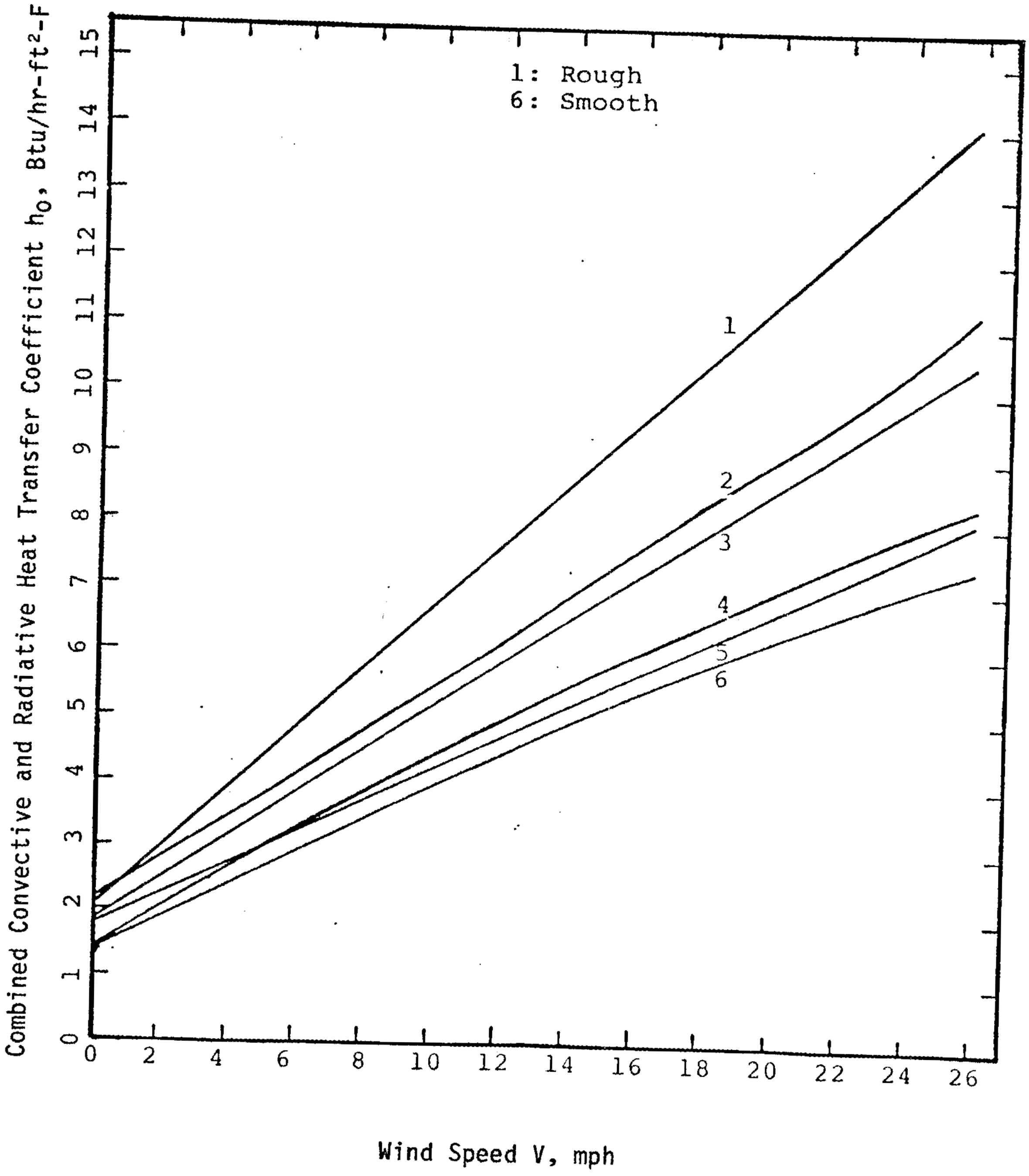

Figure C.1 Representation of Correlations for h_0 with Wind Speed Incorporated in DOE 2.1B for Different Surface Roughnesses

APPENDIX D

PRELIMINARY CALCULATIONS OF ACES AND AHEP

USING ONLY DOE 2.1B LOADS SUBPROGRAM

APPENDIX D

PRELIMINARY CALCULATIONS OF ACES AND AHEP USING ONLY DOE 2.1B LOADS SUBPROGRAM

Several preliminary runs were made using only the LOADS portion of DOE 2.1B. These were made for several reasons: (1) computer runs where only output from the LOADS program is specified run considerably faster than runs incorporating the SYSTEMS program; (2) it was desired to examine the order-of-magnitude of changes in heating and cooling loads resulting from decreasing the roof's solar absorptance for several locations as an aid in selecting locations for more extensive simulations; (3) it was reasoned that LOADS' output would serve to indicate the relative effect of the type and amount of roof insulation; (4) it was also reasoned that insight as to the role of thermal capacitance could be gained from the output of LOADS. The first set of runs was made using steady-state calculations with heat transfer occurring only through the roof. The second set of runs involved use of transient calculations in which the thermal response factors of the roof and space weighting factors were included. In an attempt, however, to otherwise focus solely on the effect of the roof, no internal loads were included and the walls and floor were specified to be adiabatic. Thus, net heat transfer with the outside was forced to occur only through the roof. In all of the calculations involving only the LOADS subprogram, the inside temperature was specified to be 74°F.

Table D.1 shows the changes in cooling and heating loads determined for U values of 0.2, 0.1 and 0.04 Btu/hr-ft^2-F using steady-state calculations. As expected, reduction of the roof's solar absorptance (0.8 to 0.3) resulted in a decrease in the cooling load and an increase in the heating load for all thirty locations examined. The results in Table D.1 have been ordered in accordance with decreasing values of the sum (ACES + AHEP). Annual cooling energy savings (ACES) is largest for locations characterized by large cooling requirements. For two locations characterized by comparable cooling requirements, ACES is larger for the one having the greater solar availability during the cooling season. Conversely, annual heating energy penalties (AHEP) due to the reduction in the roof's solar absorptance are larger for locations having large heating loads. Also as expected, the smaller U values resulted in attenuation of both ACES and AHEP. For a U value of 0.1, ACES and AHEP were lower than for U = 0.2 by a factor that ranged from 0.486 to 0.493. For U = 0.04 the factor ranged from 0.792 to 0.796. The reason that the factor was not exactly 0.5 and 0.8 is due to the variable radiative and convective surface resistance that is taken into account within the code.

Using LOADS, a series of runs was made in which the thermal capacitance of the roof was taken into account. A space was defined to be encompassed by the roof, walls and a floor. The walls and floor were forced to be adiabatic so that heat transfer occurred only through the roof. Runs were made for the same thirty locations

Table D.1. Preliminary ACES and AHEP Values from DOE 2.1B LOADS Subprogram Using Steady-State Calculations. Input Data Listed in Table D.4

	U = 0.2 Btu/hr-ft²-F			U = 0.1 Btu/hr-ft²-F			U - 0.04 Btu/hr-ft²-F		
Location	ACES (Btu/ft²)	AHEP (Btu/ft²)	ACES+AHEP (Btu/ft²)	ACES (Btu/ft²)	AHEP (Btu/ft²)	ACES+AHEP (Btu/ft²)	ACES (Btu/ft²)	AHEP (Btu/ft²)	ACES+AHEP (Btu/ft²)
Bakersfield, CA	7899	3429	11328	4046	1758	5804	1644	715	2359
Phoenix, AZ	7736	2375	11222	4509	1215	5625	1726	484	2321
Albuquerque, NM	6220	4801	11021	3180	2452	5632	1289	993	2282
El Paso, TX	7245	3210	10455	3695	1635	5330	1497	662	2159
Denver, CO	3998	4539	8537	2040	2311	4351	826	933	1759
Knoxville, TN	4153	2795	6948	2125	1428	3553	862	579	1441
San Francisco, CA	1923	4837	6760	977	2459	3436	395	992	1387
Augusta, GA	4197	3503	6700	2139	1275	3414	865	516	1381
Bangor, ME	2574	4065	6639	1321	2088	3409	537	848	1385
Atlanta, GA	4060	2501	6561	2072	1272	3344	839	514	1353
Orlando, FL	5062	1385	6447	2573	705	3278	1041	285	1326
San Antonio, TX	4672	1754	6426	2371	891	3262	958	361	1319
Memphis, TN	4032	2306	6338	2054	1174	3228	830	474	1304
Nashville, TN	3704	2528	6232	1890	1288	3178	765	521	1286
Miami, FL	5413	747	6160	2746	380	3126	1111	154	1265
Tampa, FL	4677	1434	6111	2373	729	3102	958	295	1253
Lake Charles, LA	4298	1689	5987	2188	859	3047	885	348	1233
St. Louis, MO	3426	2453	5879	1744	1246	2990	705	503	1208
Washington, DC	2981	2757	5738	1519	1404	2923	614	566	1180
Charleston, SC	3518	2172	5690	1788	1104	2892	722	447	1169
Portland, OR	2392	3064	5456	1220	1566	2786	494	633	1127
Houston, TX	3786	1515	5301	1923	768	2691	777	311	1088
Chicago, IL	2348	2724	5072	1194	1384	2578	482	558	1040
Madison, WI	1960	2909	4869	995	1481	2476	401	598	999
Indianapolis, IN	2473	2317	4790	1257	1177	2434	509	474	982
Seattle, WA	1520	3220	4740	774	1642	2416	313	663	976
Minneapolis, MN	1994	2706	4700	1012	1375	2387	409	555	964
Minot, ND	1753	2843	4596	892	1443	2335	361	582	943
Syracuse, NY	1779	2521	4300	905	1284	2189	366	519	885
New York, NY	1768	2267	4035	898	1149	2047	363	462	825

Table D.2 Preliminary ACES and AHEP Values from DOE 2.1B LOADS Subprogram Using Roof Thermal Response Factors (Roof Insulation: Fiberboard, Other Input Data Given in Table D.4)

Location	U = 0.2 Btu/hr-ft²-F			U = 0.04 Btu/hr-ft²-F		
	ACES (Btu/ft²)	AHEP (Btu/ft²)	ACES+AHEP (Btu/ft²)	ACES (Btu/ft²)	AHEP (Btu/ft²)	ACES+AHEP (Btu/ft²)
Phoenix, AZ	6701	2701	9402	1401	744	2145
Bakersfield, CA	5611	3606	9217	1084	1015	2099
Albuquerque, NM	4313	4820	9133	826	1250	2076
El Paso, TX	5431	3292	8723	1100	882	1982
Denver, CO	2594	4530	7124	410	1199	1609
Knoxville, TN	3026	2714	5740	642	667	1309
Augusta, GA	3132	2496	5628	652	632	1284
San Francisco, CA	4825	759	5584	12	1244	1256
Atlanta, GA	3012	2496	5508	626	626	1252
Bangor, ME	1475	3919	5394	154	1078	1232
San Antonio, TX	3561	1831	5392	705	516	1221
Orlando, FL	3851	1538	5389	778	445	1223
Memphis, TN	3109	2203	5312	675	532	1207
Nashville, TN	2798	2406	5204	584	600	1184
Miami, FL	4306	865	5171	921	250	1171
Tampa, FL	3531	1601	5132	679	483	1162
Lake Charles, LA	3255	1760	5015	652	488	1140
St. Louis, MO	2573	2353	4926	526	589	1115
Washington, DC	2117	2697	4814	393	699	1092
Charleston, SC	2572	2194	4766	505	577	1082
Portland, OR	1420	3096	4516	133	893	1026
Houston, TX	2917	1532	4447	591	417	1008
Chicago, IL	1702	2536	4238	331	625	956
Madison, WI	1301	2793	4092	205	721	926
Indianapolis, IN	1741	2306	4047	301	613	914
Seattle, WA	769	3181	3950	48	845	893
Minneapolis, MN	1403	2541	3944	245	646	891
Minot, ND	1170	2688	3858	179	691	870
Syracuse, NY	1141	2453	3594	154	661	815
New York, NY	1250	2128	3378	232	527	759

Table D.3 Preliminary ACES and AHEP Values from DOE 2.1B LOADS Subprogram Using Roof Thermal Response Factors (Roof Insulation: EPS, Other Input Data Given in Table D.4)

Location	U = 0.2 Btu/hr-ft²-F ACES (Btu/ft^2)	AHEP (Btu/ft^2)	ACES+AHEP (Btu/ft^2)	U = 0.04 Btu/hr-ft²-F ACES (Btu/ft^2)	AHEP (Btu/ft^2)	ACES+AHEP (Btu/ft^2)
Phoenix, AZ	6450	2664	9414	1531	639	2170
Bakersfield, CA	5677	3577	9254	1284	855	2139
Albuquerque, NM	4364	4793	9157	981	1129	2110
El Paso, TX	5470	3269	8739	1239	772	2011
Augusta, GA	3149	2485	5634	713	582	1295
San Antonio, TX	3584	1815	5399	807	429	1236
Memphis, TN	3124	2194	5318	709	512	1221
Miami, FL	4321	855	5176	981	204	1185
Tampa, FL	3556	1582	5138	798	377	1175
Lake Charles, LA	3276	1745	5021	740	413	1153
Washington, DC	2136	2684	4820	478	628	1106
Chicago, IL	1717	2524	4241	384	584	968
Indianapolis, IN	1758	2291	4049	391	534	925
Minot, ND	1185	2678	3863	261	622	883
Syracuse, NY	1160	2440	3600	253	571	824

listed in Table D.1 with the properties of fiberboard used for the roof insulation. The results are tabulated in Table D.2. Runs were made for fifteen locations with the properties of EPS instead of those for fiberboard used for the roof insulation. These results are listed in Table D.3. Table D.4 gives conditions and insulation properties used in making the transient calculations.

Table D.4 Data Used in Making the Transient LOADS Calculations

Roof Dimensions	250 ft x 250 ft
Inside Temperature	74°F
Wall Construction	4-inch face brick; air-gap; 8-inch concrete block
Floor Construction	6-inch concrete slab on grade
Roof Construction	0.5-inch layer of stones; 0.375-inch BUR; insulation; and 0.060-inch steel deck
Fiberboard Insulation	k = 0.03 Btu/hr-ft^2-F; D = 17.5 lbm/ft^3; C_p = 0.33 Btu/lbm-F
EPS Insulation	k = 0.0217 Btu/hr-ft^2-F; D = 1.0 lbm/ft^3; C_p = 0.29 Btu/lbm-F
Roof Absorptance Change	(0.8 - 0.3) = 0.5

Comparisons of the results for steady-state calculations with those for transient calculations followed expected trends. The net effect (ACES + AHEP) for the transient calculations was lower in all cases than for the corresponding steady-state calculation. For U = 0.2, the ratio of (ACES + AHEP) for steady-state calculations to that for transient calculations was approximately 1.2 for all cases whereas the ratio for U = 0.04 was approximately 1.08. The differences between ACES values as well as between AHEP values resulting from a change in insulation from fiberboard to EPS were insignificant.

APPENDIX E

BUILDING DESCRIPTIONS

APPENDIX E

BUILDING DESCRIPTIONS

Three different building descriptions were used as input to DOE 2.1B during the course of this study. Choices for two of the descriptions were made in conjunction with some other work involving DOE 2.1B simulations. All three buildings were single story having flat built-up roofs and concrete slab floors.

Building A, having a roof area of 1500 ft^2, is schematically shown in Figure E.1. It represents an interior office space located within a strip of identical contiguous units. The sides adjacent to other conditioned spaces were treated as having no heat transfer across them.

Building B, having a roof area of 10,242 ft^2, is schematically shown in Figure E.2. Building B represents an open maintenance building or light manufacturing facility.

Building C, having a roof area of 50,000 ft^2, is schematically shown in Figure E.3. Building C is a multizone building having four perimeter zones and a large open zone in the middle of the building as shown in Figure E.3.

The inside surface of the roof deck for Buildings B and C was next to the conditioned space. There was a dropped ceiling in Building A which provided an unconditioned space between the roof and the conditioned space.

In this work, roof descriptions were identical for all three buildings; however, differences were input for certain other parameters. More specific input details are given in the remainder of this appendix.

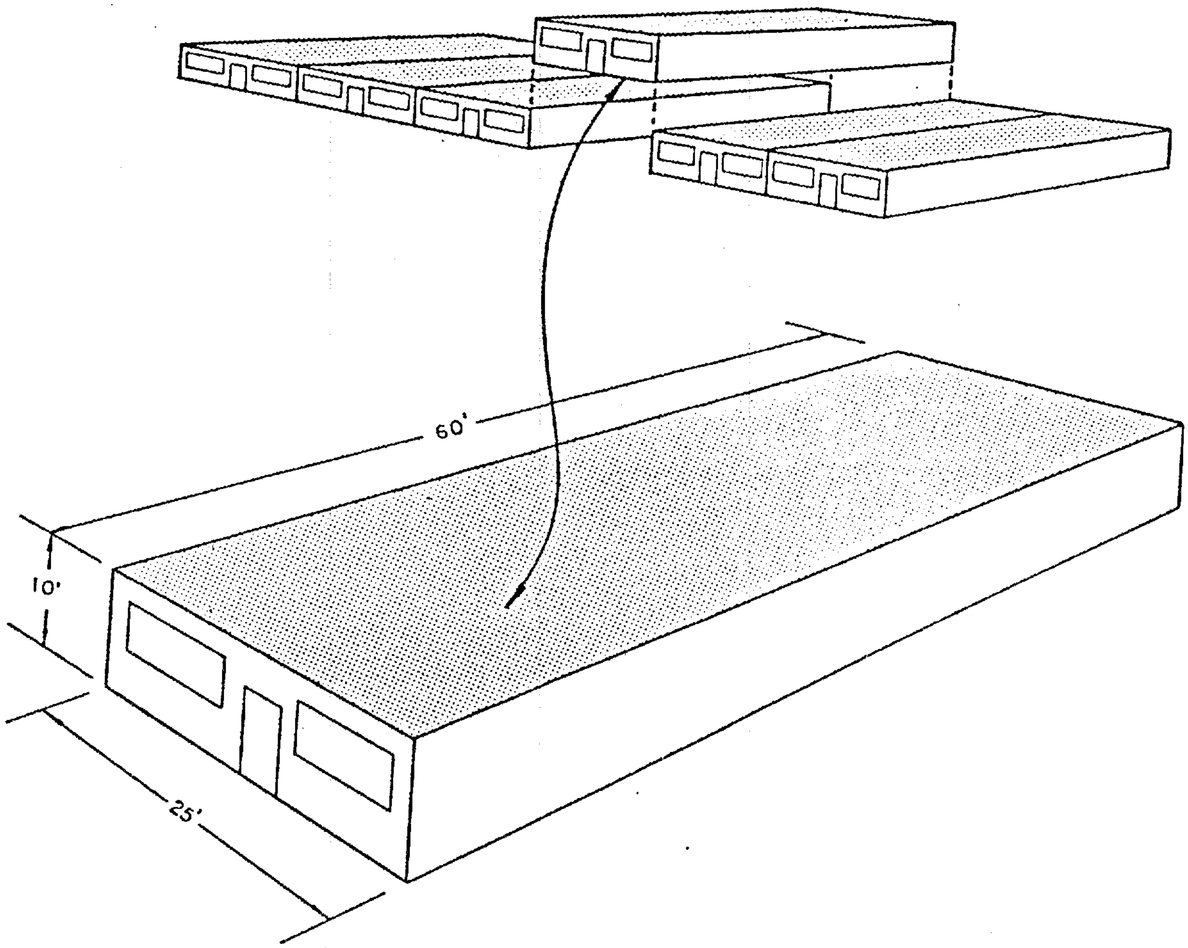

Figure E.1 Schematic of Building A

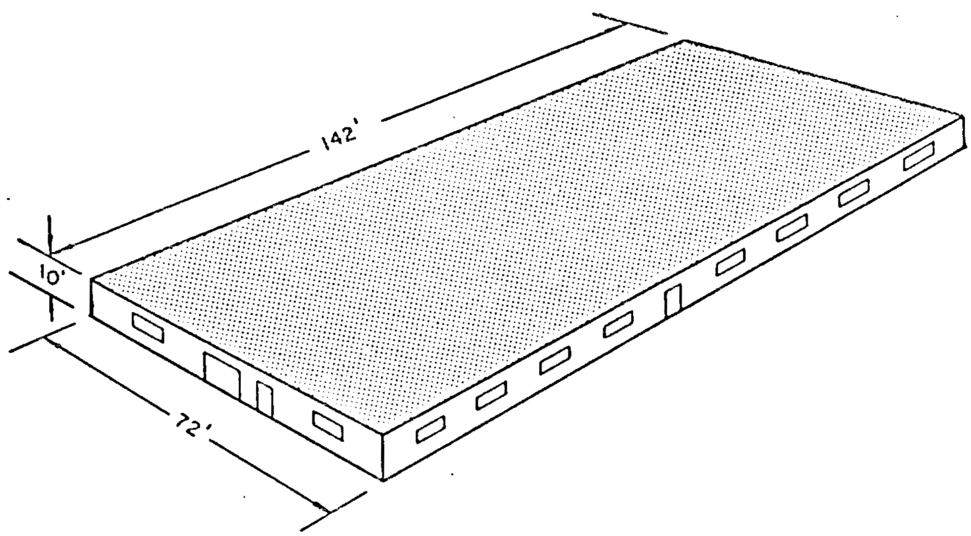

Figure E.2 Schematic of Building B

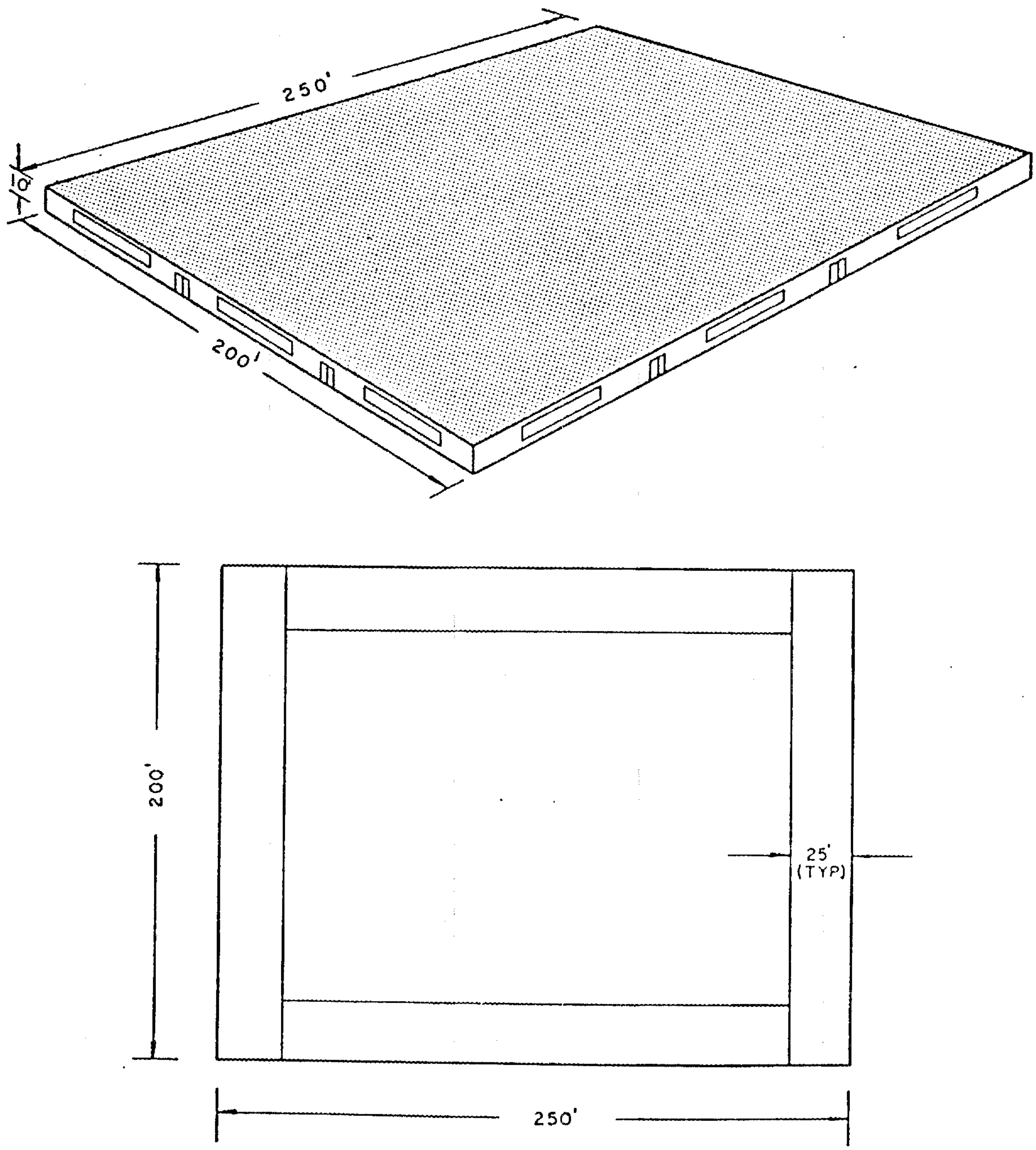

Figure E.3 Schematic of Building C

ROOF DESCRIPTION
(All Three Buildings)

Layer	L ft	k Btu/hr-ft^2-F	D lbm/ft^3	C Btu/lbmF	Thermal Resistance ft^2-hr-F/Btu
Aggregate	0.0417	0.83	55	0.40	0.050
Membrane	0.0313	0.11	70	0.40	0.283
Insulation	*	0.03	17.5	0.33	**
Steel Deck	0.005	26	480	0.10	--
Inside Film Resistance	--	--	--	--	0.192

* 0.1124, 0.2624 and 0.7124 to yield U' values of 0.2, 0, 1 and 0.04 Btu/hr-ft^2-F, respectively.

** 3.745, 8.745, and 23.745 corresponding to above thicknesses.

FLOOR DESCRIPTION

Layer	L ft	k Btu/ hr-ft^2-F	D lbm/ ft^3	C Btu/ lbmF	Thermal Resistance ft^2-hr-F/ Btu	Building
Earth	1.67	0.5	130	0.3	3.33	A, B, C
Concrete Slab	0.33	1.0	140	0.22	0.33	A, C
Concrete Slab	0.5	1.0	140	0.22	0.50	B
Inside Film Resistance	--	--	--	--	0.61	A, B, C

EXTERIOR WALL DESCRIPTION*

Layer	L ft	k Btu/ hr-ft²-F	D lbm/ ft³	C Btu/ lbmF	Thermal Resistance ft²-hr-F/ Btu	Building
Brick	0.333	0.4167	120	0.2	0.80	A, B, C
Air Gap	--	--	--	--	0.89	A, B, C
8" Concrete Block	0.667	0.3876	53	0.20	1.72	A, B, C
Insulation	0.0833	0.02	1.8	0.29	4.17	A, B
Insulation	0.1667	0.02	1.8	0.29	8.33	C
Gypsum Board	.0521	0.0926	50	0.26	0.56	A, B, C
Inside Film Resistance	--	--	--	--	0.68	A, B, C

* Solar Absorptance = 0.75 for A, B, and C. Roughness Code of 2 for B and C and 5 for A (See Appendix C).

SPACE CONDITIONS

Condition	Building A	Building B	Building C
Temperature for LOADS, °F	75	75	74
Number of People	10	20	252
People Heat Gain (Btu/person)	450	500	450
Lighting Load (W/ft²)	2.5	2.5	2.5
Equipment Load (W/ft²)	1.0	1.0	1.0
Infiltration (Air Changes/hr)	0.5	1.0	0.35
Furniture Weight per square foot	25	10	8

HVAC EQUIPMENT

	Building A	B	C
Thermostat Set Point Cooling, °F	78	78	78
Thermostat Set Point Heating, °F	72	72	72
Ventilation Air (CFM/Person)	5	7	5
Equipment	Packaged Rooftop	Packaged Rooftop	Multizone with Reheat

All windows were single pane.

Infiltration in Buildings A and B occurred throughout the year; for Building C, infiltration occurred from November through March 31.

APPENDIX F

CHANGES IN ANNUAL BUILDING ENERGY REQUIREMENTS COMPUTED BY DOE 2.1B FOR BUILDINGS A & B CORRESPONDING TO A REDUCTION IN SURFACE ABSORPTANCE FROM 0.8 to 0.3

APPENDIX F

CHANGES IN ANNUAL BUILDING ENERGY REQUIREMENTS COMPUTED BY DOE 2.1B FOR BUILDINGS A & B CORRESPONDING TO A REDUCTION IN SURFACE ABSORPTANCE FROM 0.8 to 0.3

Tabulated in this appendix for reference purposes are the values predicted for changes in building energy requirements for Buildings A and B. Building descriptions are given in Appendix E. In each table, the results have been ordered in accordance with descending values of the sum (ACES + AHEP).

Table F.1 Predicted Changes in Annual Energy Requirements for Building A (U' = 0.2 Btu/hr-ft²-F; Roof's α Reduced from 0.8 to 0.3)

Location	ACES	AHEP	ACES+AHEP	Electrical Energy Savings Cool. Syst. Input	Fan
	Btu/ft²	Btu/ft²	Btu/ft²	KwHr	KwHr
Phoenix, AZ	6520	117	6637	1341	60
Bakersfield, CA	5440	228	5668	1154	33
El Paso, TX	5061	300	5361	1074	52
Albuquerque, NM	3977	783	4760	885	29
Miami, FL	3901	17	3918	755	32
Tampa, FL	3778	80	3858	739	28
San Antonio, TX	3581	157	3738	685	34
Denver, CO	2513	1091	3604	623	20
Augusta, GA	3212	291	3503	763	23
Memphis, TN	3077	395	3472	602	23
Lake Charles, LA	3281	115	3396	453	2
St. Louis, MO	2589	597	3186	557	12
Washington, DC	2296	662	2958	420	9
Chicago, IL	1779	800	2579	317	7
Indianapolis, IN	1778	607	2385	326	7
Minneapolis, MN	1425	887	2312	264	- 1
Minot, ND	1232	916	2148	271	- 1
Syracuse, NY	1315	700	2015	235	1
Portland, OR	1582	413	1995	249	3
Seattle, WA	1065	508	1573	183	- 3

Table F.2 Predicted Changes in Energy Requirements for Building A (U' = 0.2 Btu/hr-ft²-F; Roof's α Reduced from 0.3 to 0.3)

Location	ACES	AHEP	ACES+AHEP	Electrical Energy Savings Cool. Syst. Input	Fan
	Btu/ft²	Btu/ft²	Btu/ft²	KwHr	KwHr
Phoenix, AZ	3665	101	3766	795	59
Bakersfield, CA	2979	180	3159	416	23
El Paso, TX	2778	182	2960	416	25
Albuquerque, NM	2089	483	2572	398	23
Miami, FL	2253	17	2270	361	21
Tampa, FL	2140	51	2191	592	32
San Antonio, TX	1961	122	2083	566	43
Augusta, GA	1827	176	2003	224	6
Lake Charles, LA	1889	104	1993	168	3
Memphis, TN	1761	212	1973	388	28
Washington, DC	1237	252	1589	171	6
Chicago, IL	966	432	1398	433	22
Indianapolis, IN	968	320	1288	342	23
Minot, ND	620	542	1162	129	- 2
Syracuse, NY	708	391	1099	114	- 2

Table F.3 Predicted Changes in Energy Requirements for Building A ($U' = 0.04$ Btu/hr-ft^2-F; Roof's α Reduced from 0.8 to 0.3)

Location	ACES	AHEP	ACES+AHEP	Electrical Energy Savings	
				Cool. Syst. Input	Fan
	Btu/ft^2	Btu/ft^2	Btu/ft^2	KwHr	KwHr
Phoenix, AZ	1533	55	1588	270	33
Bakersfield, CA	1190	83	1273	199	23
El Paso, TX	1161	103	1264	181	20
Miami, FL	1071	4	1075	156	20
Albuquerque, NM	824	246	1070	120	15
Tampa, FL	930	23	953	134	15
San Antonio, TX	886	58	944	123	12
Augusta, GA	853	90	943	139	16
Lake Charles, LA	861	42	903	140	17
Memphis, TN	789	108	897	128	15
Washington, DC	532	165	697	75	5
Chicago, IL	406	185	591	54	2
Indianapolis, IN	419	151	570	58	4
Minot, ND	249	261	510	30	- 1
Syracuse, NY	263	186	449	31	- 2

Table F.4 Predicted Changes in Energy Requirements for Building B, Case B1 (U' = 0.2 Btu/hr-ft²F; Roof's α Reduced from 0.8 to 0.3)

Location	ACES	AHEP	ACES+AHEP	Electrical Energy Savings Cool. Syst. Input	Fan
	Btu/ft²	Btu/ft²	Btu/ft²	KwHr	KwHr
Phoenix, AZ	5581	417	5998	8385	3261
El Paso, TX	4714	1086	5800	6242	4332
Memphis, TN	4298	955	5253	4696	2025
Bakersfield, CA	4546	685	5231	6277	3113
Albuquerque, NM	3116	1903	5019	3654	1716
Miami, FL	4851	34	4885	5493	1398
Lake Charles, LA	4054	372	4426	5058	1873
Tampa, FL	4094	174	4268	4666	1328
San Antonio, TX	3692	426	4118	4646	1680
Augusta, GA	2705	787	3492	3503	1275
Washington, DC	2227	1188	3415	2619	1434
Chicago, IL	1725	1216	2941	1735	872
Indianapolis, IN	1681	1176	2857	1855	1604
Syracuse, NY	1255	971	2226	1170	456
Minot, ND	800	1212	2012	809	- 132

Table F.5 Predicted Changes in Energy Requirements for Building B, Case B1 (U' = 0.1 Btu/hr-ft²-F; Roof's α Reduced from 0.8 to 0.3)

Location	ACES	AHEP	ACES+AHEP	Electrical Energy Savings Cool. Syst. Input	Electrical Energy Savings Fan
	Btu/ft²	Btu/ft²	Btu/ft²	KwHr	KwHr
Phoenix, AZ	2859	152	3011	3715	1388
El Paso, TX	2427	395	2822	3297	1968
Bakersfield, CA	2347	254	2601	3319	1825
Miami, FL	2464	10	2473	2756	679
Lake Charles, LA	2286	149	2435	2885	1033
Albuquerque, NM	1598	808	2406	1785	753
San Antonio, TX	2033	178	2211	2485	804
Tampa, FL	2021	64	2085	2271	629
Washington, DC	1214	558	1772	1296	643
Indianapolis, IN	1216	487	1703	1134	573
Memphis, TN	1232	401	1633	1924	973
Augusta, GA	1187	330	1517	1705	640
Syracuse, NY	721	447	1168	645	68
Chicago, IL	480	596	1076	621	496
Minot, ND	411	571	982	398	-126

Table F.6 Predicted Changes in Energy Requirements for Building B, Case B1 ($U' = 0.04$ Btu/hr-ft^2-F; Roof's α Reduced from 0.8 t 0.3)

Location	ACES Btu/ft^2	AHEP Btu/ft^2	ACES+AHEP Btu/ft^2	Electrical Energy Savings: Cool. Syst. Input KwHr	Electrical Energy Savings: Fan KwHr
Memphis, TN	1406	142	1548	1173	242
Phoenix, AZ	1209	51	1260	1638	865
Miami, FL	1079	3	1082	1184	269
El Paso, TX	907	141	1048	1180	564
Bakersfield, CA	966	71	1037	1257	669
San Antonio, TX	819	70	889	996	303
Albuquerque, NM	535	305	840	596	236
Lake Charles, LA	780	47	827	893	256
Chicago, IL	569	214	783	435	130
Tampa, FL	740	22	762	749	171
Washington, DC	415	193	608	385	143
Minot, ND	176	239	415	167	- 47
Indianapolis, IN	238	160	398	225	83
Augusta, GA	122	99	221	385	148
Syracuse, NY	50	154	204	88	- 30

Table F.7 Predicted Changes in Energy Requirements for Building B, Case B2 (U' = 0.2 Btu/hr-ft²-F; Roof's α Reduced from 0.8 to 0.3)

Location	ACES	AHEP	ACES+AHEP	Electrical Energy Savings	
				Cool. Syst. Input	Fan
	Btu/ft²	Btu/ft²	Btu/ft²	KwHr	KwHr
Phoenix, AZ	5181	331	5512	5746	918
El Paso, TX	4272	745	5017	4625	923
Bakersfield, CA	4224	539	4763	4810	843
Albuquerque, NM	2992	1645	4637	3124	80
Miami, FL	4136	29	4165	3955	457
Memphis, TN	3241	720	3961	3290	342
Augusta, GA	3096	679	3775	3271	341
Tampa, FL	3623	144	3767	3577	357
Lake Charles, LA	3403	277	3680	3453	388
San Antonio, TX	3260	348	3608	3517	445
Washington, DC	2051	945	2996	2021	59
Chicago, IL	1393	1037	2430	1357	16
Indianapolis, IN	1557	864	2421	1481	39
Minot, ND	852	1217	2069	844	-113
Syracuse, NY	1009	868	1877	960	- 51

Table F.8 Predicted Changes in Energy Requirements for Building B, Case B3 (U' = 0.2 Btu/hr-ft^2-F; Roof's α Reduced from 0.8 to 0.3)

Location	ACES	AHEP	ACES+AHEP	Electrical Energy Savings Cool. Syst. Input	Electrical Energy Savings Fan
	Btu/ft^2	Btu/ft^2	Btu/ft^2	KwHr	KwHr
Phoenix, AZ	6078	497	6575	6199	0
Miami, FL	6382	92	6474	5945	0
El Paso, TX	5167	1262	6429	5039	0
Lake Charles, LA	5504	487	5991	5083	0
Albuquerque, NM	3544	2271	5815	3684	0
Bakersfield, CA	4693	963	5656	5991	0
Memphis, TN	4489	1114	5603	4197	0
Tampa, FL	5174	322	5296	4736	0
Augusta, GA	3976	960	4936	3947	0
Denver, CO	2325	2513	4838	2461	0
San Antonio, TX	3869	594	4463	4046	0
Washington, DC	3105	1321	4426	2949	0
St. Louis, MO	3190	1186	4376	2949	0
Indianapolis, IN	2401	1152	3553	2499	0
Chicago, IL	2121	1379	3500	2252	0
Minneapolis, MN	1766	1530	3296	1826	0
Syracuse, NY	1675	1238	2913	1762	0
Portland, OR	1632	1210	2842	2842	0
Minot, ND	1170	1617	2787	1273	0
Seattle, WA	833	1704	2537	927	0

Table F.9 Predicted Changes in Energy Requirements for Building B, Case B4 (U' = 0.2 Btu/hr-ft²-F; Roof's α Reduced from 0.8 to 0.3)

Location	ACES	AHEP	ACES+AHEP	Electrical Energy Savings	
				Cool. Syst. Input	Fan
	Btu/ft^2	Btu/ft^2	Btu/ft^2	KwHr	KwHr
Phoenix, AZ	9777	888	10665	10003	0
Miami, FL	10322	149	10471	9218	0
El Paso, TX	8191	1835	10026	7862	0
Lake Charles, LA	8709	766	9475	7926	0
San Antonio, TX	8404	929	9333	7770	0
Albuquerque, NM	5816	3313	9129	5777	0
Tampa, FL	8438	514	8952	7178	0
Memphis, TN	7035	1772	8807	6587	0
Bakersfield, CA	7421	1309	8730	7887	0
Augusta, GA	6775	1522	8297	6913	0
Denver, CO	3809	3708	7517	3955	0
St. Louis, MO	5498	1868	7366	5133	0
Washington, DC	4913	2100	7013	4560	0
Indianapolis, IN	3906	1382	5738	3927	0
Chicago, IL	3435	2226	5661	3513	0
Minneapolis, MN	2976	2429	5204	3033	0
Minot, ND	2196	2642	4838	2209	0
Syracuse, NY	2671	1937	4608	2757	0
Portland, OR	2664	1761	4425	2791	0
Seattle, WA	1352	2421	3773	1463	0

TM-10339

INTERNAL DISTRIBUTION

1. R. S. Carlsmith
2. J. E. Christian
3. G. E. Courville
4. F. A. Creswick
5. W. Fulkerson
6. M. A. Kuliasha
7. D. L. McElroy
8. H. McLain
9. W. R. Mixon
10. D. E. Reichle
11. E. Rogers
12-26. S. D. Samples
27. J. P. Sanders
28. R. B. Shelton
29-31. Laboratory Records
32. Laboratory Records (RC)
33. ORNL Patent Office
34. Y-12 Technical Library
35. Central Research Library
36. Document Reference Section

EXTERNAL DISTRIBUTION

37. R. L. Alumbaugh, Naval Civil Engineering Lab., Port Hueneme, CA
38. E. L. Bales, New Jersey Institute of Technology, Newark, NJ
39. J. V. Beck, Michigan State University, E. Lansing, MI
40. J. J. Boulin, DOE/CE, Washington, DC
41. J. H. Cable, Cable Associates, Inc., Alexandria, VA
42. W. Carroll, Lawrence Berkeley Laboratory, Berkeley, CA
43. J. J. Cuttica, Gas Research Institute, Chicago, IL
44. J. G. Driggans, TVA, Chattanooga, TN
45. W. P. Ellis, Standards Consultant, Harleysville, PA
46. D. M. Evans, Jr., Steven Winter Associates, Inc., New York, NY
47. P. W. Fairey, III, Florida Solar Energy Center, Cape Canaveral, FL
48. H. A. Fine, 949 Wishbone Circle, Lexington, KY
49. W. R. French, Moisture Systems, Incorporated, Houston, TX
50. C. F. Gilbo, Journal of Thermal Insulation, Lancaster, PA
51. W. P. Goss, University of Massachusetts, Amherst, MA
52. E. I. Griggs, Tennessee Technological University, Cookeville, TN
53. D. A. Harris, NIBS, Washington, DC
54. R. Hauser, Hauser Laboratories, P.O. Box G, Boulder, CO
55. E. Johannes, EFCG, U.S. Department of Energy, Bonneville Power Administration, Portland, OR

56. J. P. Kalt, Harvard University, Cambridge, MA
57. W. M. Kroner, Rensselaer Polytechnic Institute, Troy, NY
58. R. A. LaCosse, National Roofing Contractors Assn., Rosemont, IL
59. E. Leger, P. O. Box 549, New Boston, NH
60. R. A. Lucas, Tremco, Lexington, MA
61. R. Mack, Dow Chemical, Freeport, TX
62. P. C. Martin, Manville Sales Corporation, Denver, CO
63. J. McCorkle, 6720 S. Steele Street, Littleton, CO
64. D. McGuire, Regal Industries, Crothersville, IN
65. G. Miller, Jim Walter Research Corp., St. Petersburg, FL
66. M. Millspaugh, Reflectixs, Inc., Markleville, IN
67. D. E. Morrison, Michigan State University, E. Lansing, MI
68. P. G. Mulroney, 4557 King Edward Court, Annandale, VA
69. J. R. Mumaw, Owens-Corning Fiberglas, Granville, OH
70. E. Nowman, Fi-Foil Company, Inc., Auburndale, FL
71. R. E. Oliver, DOE/CE, Washington, DC
72. R. L. Perrine, University of California, Los Angeles, CA
73. F. J. Powell, 9919 Mayfield Drive, Bethesda, MD
74. D. E. Richards, Owens-Corning Fiberglas, Toledo, OH
75. W. J. Rossiter, NIST, Gaithersburg, MD
76. J. Samos, NASA - Langley, Hampton, VA
77. E. Schaffer, U.S. Forest Products Lab, Madison, WI
78. W. W. Seaton, ASHRAE, Atlanta, GA
79. S. Selkowitz, Lawrence Berkeley Laboratory, Berkeley, CA
80. W. Shaw, Harcourt Brace Jovanovich Publications, Cleveland, OH
81. M. Sherman, Jim Walter Corporation, St. Petersburg, FL
82. P. H. Shipp, USG Corporation, Libertyville, IL
83. C. J. Shirtliffe, National Research Council, Ottawa, Ontario, Canada
84. D. R. Smith, NIST, Boulder, CO
85. H. S. Smith, Cellin Manufacturing Inc., Lorton, VA
86. S. E. Smith, Holometrix, Inc., Cambridge, MA
87. L. G. Spielvogel, Wyncote House, Wyncote, PA
88. R. Sterling, University of Minnesota, Minneapolis, MN
89. G. A. Tsongas, Portland State University, Portland, OR
90. A. Tuluca, Steven Winter Associates, Norwalk, CT
91. M. G. Van Geem, Construction Technology Laboratories, Inc., Skokie, IL
92. C. R. Vander Linden, Vander Linden & Associates, Littleton, CO
93. J. R. Warner, ACEC Research and Management Foundation, Washington, DC
94. D. Whitaker, Lescher and Mahoney, Inc., Phoenix, AZ
95. D. W. Yarbrough, Tenn. Tech. Univ., Cookeville, TN
96. Office, Assistant Manager, Energy Research and Development, DOE/ORO, Oak Ridge, TN

97-106. Office of Scientific and Technical Information, U.S. Department of Energy, Oak Ridge, TN